Bachelor thesis

INVESTIGATION OF SUB-SURFACE OCEAN INDUCTION ON JUPITER'S ICY MOON EUROPA

Student: **Cornelia Ekvall**

Abstract

Following previous studies, a theoretical model for the induced magnetic field by Europa, one of Jupiter's icy moons, is presented. The aim of the model is to find evidence for the existence of a sub-surface ocean on the moon. Moreover, the accuracy of the theoretical model is evaluated using data from the Galileo space probe and a discussion of improvements, with the upcoming mission JUICE in mind, is given.

The magnetic field from Jupiter is modeled using a dipole field and the moon is assumed to have the properties of a perfect homogeneous conductive layer (i.e a superconductor with no resistance). Europa is assumed to possess an electrically conductive subsurface ocean with conductivity σ. As the moon orbits Jupiter, the moon will experience a time-varying magnetic field since the magnetic dipole axis is tilted with an angle with respect to the rotation axis of the planet. The fact that the moon experiences a time-varying magnetic field will cause an inductive response inside the moon if a conductive material is present.

However, since this set-up reflects the ideal case, a discussion of constraints and improvements is submitted as a compliment. This thesis shows that the ocean model for Europa is supported, but further evidence is needed to fully understand the structure of the moon. The model shows a clear induction in almost all Galileo-flybys investigated, especially flyby E4 and E14. Thereby, it can be argued that the model gives a representative picture of the true induced magnetic field, with room for improvement.

In conclusion, further data is needed to fully reveal the structure of the moon, a fact that lays the foundation for the coming JUICE mission. JUICE will study both the magnetic and the electric field of Jupiter, and analyze the inner structures of the Galilean moons with higher precision than ever done before using low-frequency analysis.

Sammanfattning

Sammanfattninngsvis, med utgångspunkt i tidigare studier presenteras en modell för det inducerade magnetfältet från Jupiters isiga måne Europa. Modellens syfte är att kartlägga bevis för ett hav under ytan på månen. Fortsättningsvis diskuteras modellens noggrannhet med hjälp av data insamlat av Galileo-sonden på 90-talet tillsammans med en diskussion om den kommande JUICE-missionen.

Jupiters magnetfält kan beskrivas med hjälp av en magnetisk dipol och månen antas ha ett homogent ledande lager. Då den magnetiska dipolen ligger med en vinkel mot planetens rotation upplever månen ett tidsvarierande magnetiskt fält när den roterar runt planeten. Det tidsvarierande magnetfältet möjliggör en mätbar induktion från månen, om ett ledande material finns.

Då detta system reflekterar det ideala fallet presenteras en diskussion om begränsningar och förbättringar av modellen. Europa antas ha ett hav med konduktivitet, σ. Denna studie visar, tillsammans med tidigare studier, att det troligtvis finns ett flytande vattenlager under ytan på Europa, men att mer forskning behövs för att bestämma tjockleken och konduktiviteten av det ledande lagret bättre. Modellen valideras med hjälp av data från Galileo-sonden, där en tydlig induktion går att avläsa bland annat för förbiflygning E4 och E14.

Sammanfattningsvis visar modellen på en stark överensstämmelse med tidigare insamlad data, men vidare forskning behövs för att kunna bestämma månens struktur bättre. Med det sagt är modellen som presenteras i denna uppsats en bra utgångspunkt för den kommande JUICE missionen, som framförallt kommer studera magnetfältens interaktion med hjälp av låg-frekvensanalys.

Contents

1 Introduction **1**

2 Background **2**
2.1 The Jovian system . . . 2
2.2 Early studies of electromagnetic induction in planets . . . 2
2.3 Previous research and observations . . . 3
2.4 Overview of the method . . . 3
2.5 The environment of Europa . . . 3
2.6 Coordinate systems . . . 4
2.7 A magnetic dipole field . . . 4

3 The induction method **6**
3.1 A time-varying magnetic field . . . 6
3.2 The induced magnetic field from a uniformly conducting shell . . . 7
3.3 Equations for the magnetic field model . . . 8
3.4 Total magnetic field . . . 8
3.5 Magnetic field equations in frequency domain . . . 9
3.6 Skin depth and conductivity . . . 10
3.7 The trajectory of the spacecraft . . . 10
3.8 Determination of closest approach . . . 10
3.9 Estimation of the Jovian background field at the space craft . . . 10
3.10 Magnetic field strength depending on the conductivity and shell thickness . . . 11

4 Analysis and results **13**
4.1 Definition variables . . . 13
4.2 Data extraction and management . . . 13
4.3 Trajectories of the spacecraft relative to Europa . . . 13
4.4 The time-varying field for a synodic period . . . 13
4.5 Interaction with plasma . . . 15
4.6 The modeled magnetic field . . . 15
4.7 The inductive response depending on the conductivity . . . 16
4.8 The inductive response depending on the thickness of the conductive layer . . . 17
4.9 Constraints of the amplitude (A) and phase lag (ϕ) . . . 17
4.10 The influence of a conductive core/mantel or ionosphere . . . 20
4.11 Limitations and improvements of the model . . . 21

5 Summary, conclusion and outlook **22**

References **24**

6 Appendix **26**
6.1 Modelled field and data comparison for flyby E11, E12, E14, E15 and E19 . . . 26
6.2 Matlab code . . . 27
6.2.1 Main script . . . 27
6.2.2 Comparison of model and data . . . 32
6.2.3 Function to calculate theoretical background field . . . 36
6.2.4 Function to calculate the induced field . . . 36
6.2.5 Script to change the ammplitude factor, A . . . 37
6.2.6 Script to change the conductivity of the conductive layer . . . 40
6.2.7 Script to change the shell thickness . . . 43
6.2.8 Script to plot the flybys relative Europa . . . 46
6.2.9 Script to plot one flyby relative to Europa, in the xy-plane . . . 47

1 Introduction

This project aims to model the magnetic field from Jupiter and from the model, estimate the induced field at Europa, one of Jupiter's icy moons. With this in mind, the physics of induction and electromagnetic field theory will lay the foundation of the method and analysis. The magnetic field from Jupiter will be modeled using a dipole field and the induction will be assumed to be instantaneous. In this regard, Europa is assumed to possess an electrically conductive subsurface ocean which we will model as a homogeneous conductive layer of conductivity σ.

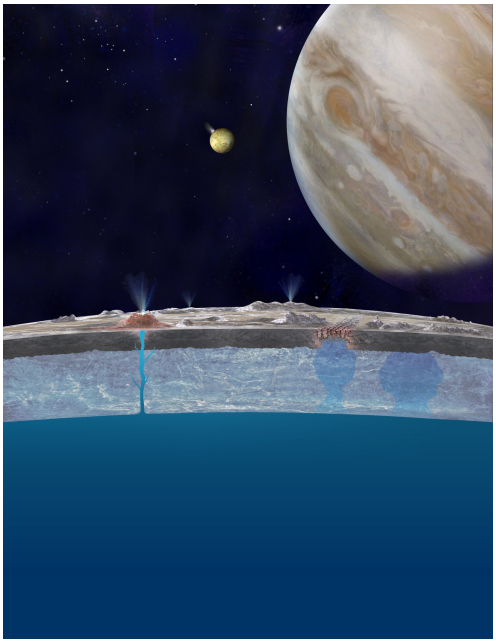

Figure 1: Below the surface of Europa, one of the Galilean moons, an ocean could exist heated by internal mechanism [NASA/JPL-Caltech, 2013].

If such a layer exists, an inductive response could be possible to observe in measurements of the magnetic and electric field by a spacecraft flying by the moon, and such induction could be explained by the presence of an ocean layer with salts. The detection of sub-surface oceans is of high interest since if heating mechanisms sustaining the liquid ocean are present, the moon could be an ideal host for microbial life. An example of such a system is shown in figure 1.

To search for sub-surface oceans in-situ (on-site) measurements are effective since they can investigate the interaction between magnetic and electric fields directly at the location. In figure 2, an illustration of a spacecraft flying past Europa is shown. In the figure, an illustration of the suggested conductive sheet (i.e. a sub-surface ocean) inside the moon is shown, together with the field lines from the induced magnetic field. The figure is obviously not to scale but gives an overview of the intention behind the model formulated in the thesis, and one of the plausible explanations of the induction measured by the Galileo space probe in the 90s.

The JUpiter ICy moons Explorer (**JUICE**) spacecraft mission will re-visit the Jovian system to once and for all determine the nature of the planets' icy moons. JUICE will arrive at Jupiter around 2031. In this work, we explore the possibility of a very simple model of oceanic induction for interpretation of the future data from JUICE.

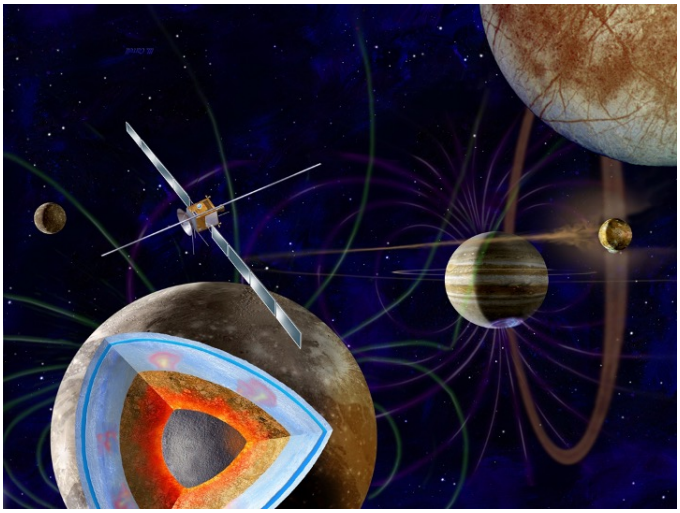

Figure 2: The figure illustrates the Jovian system, with Jupiter to the right in the background and Europa to the left with its different layers exposed. Also, a spacecraft traveling past the moon is illustrated, showing how in-situ measurements can, and have been, done. Please note that the figure is not to scale, but gives a possible interpretation of the interaction between Jupiter's magnetic field and its moons [Grasset et al., 2009]

2 Background

2.1 The Jovian system

Jupiter is the largest planet in our solar system, a giant sphere of gas, which has collected and formed many moons simultaneously with its formation billions of years ago; the four largest moons are called the Galilean moons (Ganymede, Europa, Callisto, and Io). The Jovian system is of high interest to study, not only for its own sake but also since it is expected to be similar to many systems we observe in the universe. Likewise, the coupling between the larger moons and Jupiter's magnetosphere is very interesting to investigate both in its own right, as well as it can reveal information about the structure of the moons that otherwise would be impossible to detect from Earth, without actually landing on the moons and drilling into the surface.

Each moon has different conditions and therefore has to be discussed independently. This study focuses on Europa and indirectly explores the possibility of the moon hosting life [Hussmann et al., 2014]. Europa is a good candidate for hosting life since it is believed that the moon possesses a sub-surface ocean, with heating underwater structures (such as underwater volcanoes). Also, the moon is at a distance from Jupiter, possibly immersed by the plasma from Io, where the dipole field from Jupiter can be well approximated as a perfect dipole, making it a perfect candidate to study. When studying, for instance, Ganymede's or I0, factors such as the dragged-out Jovian magnetic field, Io's volcanic activities, or Ganymede's intrinsic magnetic field, all play crucial roles. ESA's mission JUICE will explore such characteristics further, and search for oceans below the surface on all moons by studying both the magnetic and electric fields. However, this study uses data from the Galileo probe, which only measured the magnetic field, as a preparation.

2.2 Early studies of electromagnetic induction in planets

The interaction between the magnetic field of planets and moons can be described with the help application of electromagnetic induction. Arthur Schuster was the first person to describe the basic principles of electromagnetic induction in the context of planetary magnetic fields at the end of the nineteenth century. With the help of Gauss's *general theory of geomagnetism*, he showed that the observed variations in data collected at observatories on Earth's surface could be divided into internal and external parts. Schuster continued his investigation and came to the conclusion that the internal mechanism arose due to eddy currents inside the conductive material. Continuing on the path laid out by Schuster, Chapman realized that the conductivity of Earth is not uniform, in fact, it increases with depth. Furthermore, together with Whitehead, he showed that the conductive

property of Earth's ocean significantly changes the model of the interior magnetic field [Khurana et al., 2009].

2.3 Previous research and observations

Previous research has implied that a sub-surface ocean may exist below the surface of Europa, one of Jupiter's Galilean moons. Research from Galileo Doppler data [Anderson et al., 1997] showed that the measured moment of inertia was actually smaller than expected, a deviation that could be explained by a denser interior compared to the exterior. This result suggested the existence of a sub-surface ocean. Anderson et al. [1997] concluded that the most plausible model consisted of a water layer (estimated to be between 80-170 km thick) with a metallic core and a rocky mantle [Khurana et al., 2009]. Furthermore, the existence of a subsurface ocean is supported by the fact that the tidal stressing of the interior is a sufficient heat source for maintaining a liquid sub-surface ocean [Shoemaker and Wolfe, 1982].

In the 90s, the Galileo spacecraft traveled past Jupiter and its Galilean moons eleven times, measuring the magnetic field strength using a magnetometer. However, the data from three of the flybys were lost due to technical issues, and only five met the requirement for sufficient measurements and resolution to distinguish the presence of induction. The flybys E4 and E14 laid the foundation of the suspicion of an oceanic layer below the surface of Europa, first formulated by Khurana et al. [1998b] and Kivelson et al. [1999]. From flyby E26, it could be confirmed that the inductive response was in fact from a time-varying field of Jupiter and not from a tilted internal (constant) dipole [Kivelson et al., 2000]. Furthermore, the data from the Galileo probe indicated that Ganymede and Io, in contrast to Europa and Callisto, might possess internal magnetic fields [Khurana et al., 1998a].

Several models have been produced to explore the possibilities of induction from a sub-surface ocean. Furthermore, Kivelson et al. [2000] introduced a simple model for plasma correction, to discuss the limitations of plasma disturbances. The model assumes that moon and plasma interaction currents will only (or rather mainly) produce a compressional signal and will, thereby, not cause any disturbances in the magnetic field, in the equatorial plane of the moon. Also, Zimmer et al. [2000] sets the phase lag, ϕ, to be zero. In other words, the field is assumed to be induced instantaneously (not the case in reality).

In the article *Evidence for a subsurface ocean on Europa*, further evidence for Europa possessing a sub-surface ocean is presented. Using spectroscopy and gravity data, the idea of Europa has an icy crust was aided. The study estimated that the crust is about 150 km thick, with a liquid water layer below [Carr and Chapman, 1998].

2.4 Overview of the method

The method used in this thesis relies on the mechanisms of induction and the fact that a time-varying magnetic field will result in currents inside a conductive material. This means that there will be an induced field from the moon if it consists of a conductive layer, as it orbits the planet (since the magnetic field from the planet changes with respect to time from the perspective of the moon). Characteristics such as the size, structure, and conductivity of the material will affect the magnitude of the inductive response. The method is described in detail in section 3.

2.5 The environment of Europa

Europa is one of Jupiter's icy moons. But the structure of the moon below the surface is not entirely known. Previous studies, using the Galileo space probe spectra, have indicated distortions in several of the absorption bands (for water and ice), in the range from 1-3 μm. The distortions could possibly be explained by the presence of hydrated compounds, for instance by a mixture of hydrated salts and sulphuric acid hydrates. There is unfortunately no current identification of non-water/ice compounds on the moon, and further research is needed.

Furthermore, both Voyager and Galileo data have alluded to the habitability of Europa. But the depth and conductivity of the conductive layer are still unknown, and the possibility of a liquid water ocean needs to be investigated further [Hussmann et al., 2014].

The environment around a conductor will change the properties and strength of the induced field. Jupiter's magnetosphere stretches quite far, and both Europa and Callisto are located in the inner magnetosphere of the gas giant. Europa is in fact located at the outer edge of Io's plasma torus, where the plasma sheet is thin and dependent on Io. Moreover, since the dipole axis of Jupiter is tilted by 9.6° (θ in figure 3)relative to the planet's rotation axis, Europa will experience a plasma sheet which is moving up and down, depending on the synodic period of Jupiter [Khurana et al., 2009]. This means that the moons will experience the time-variation from Jupiter's magnetic field, a "wobble", and Eddy currents will therefore be produced inside the conductors, opposing the change that first induced the currents. The eddy currents will result in perturbations of the measured field close to the moon [Khurana et al., 1998b].

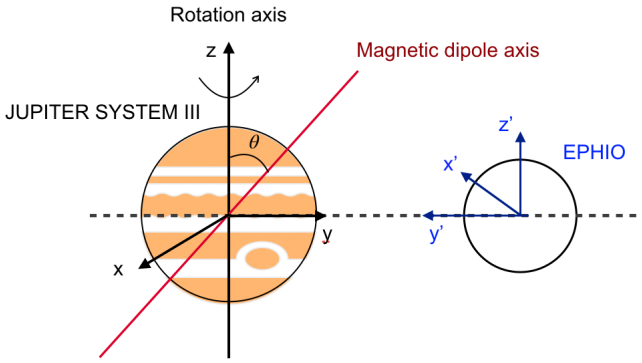

Figure 3: The definition of Jupiter system III and EPHIO system, both showing right-handed coordinate systems.

Another important realization is the fact that the plasma around the moon will move at a greater velocity (flow velocity) than the moon (Kepler velocity), leading to a process called **co-rotation**.

2.6 Coordinate systems

To describe the modeled magnetic field, two coordinate systems are used in this study, one which is Jupiter-centered (Jupiter System III) and another which is Europa-centered (EPHIO). The two coordinate systems are illustrated in figure 3 and are also described below in table 1.

Table 1: The coordinate systems used in this thesis are defined below, both right-handed.

direction	Jupiter System III	EPHIO
x-axis	$\mathbf{x}=(\mathbf{y} \times \mathbf{z})$	$\mathbf{x}=(\mathbf{y} \times \mathbf{z})$
y-axis	pointing towards Europa $(\mathbf{z} \times \mathbf{x})$	pointing towards Jupiter
z-axis	parallel to the rotation axis of Jupiter	parallel to the rotation axis of Jupiter

Furthermore, to test the model, data from the Galileo space probe is used. The Galileo space probe did flybys of Europa on the 4th, 11th, 12th, 14-19th orbit of Jupiter in October 1999, and they are labeled as follows: E4, E6, E11 and E14-E19. However, the data from flybys E6, E16 and E18 were lost due to technical errors. In this investigation, we will consider the system illustrates in figure 4, where the spacecraft travels close to the moon, in a short period of time.

2.7 A magnetic dipole field

To understand the mechanism behind magnetic fields in space, we turn to the basic principles of electricity and magnetism. The general form of a dipole field can be written as, in SI-units, [Nordling and Österman, 2020]:

$$\mathbf{B}_{dipole} = C[(\mathbf{r} \cdot \mathbf{M}) - r^2\mathbf{M}]/r^5 \tag{1}$$

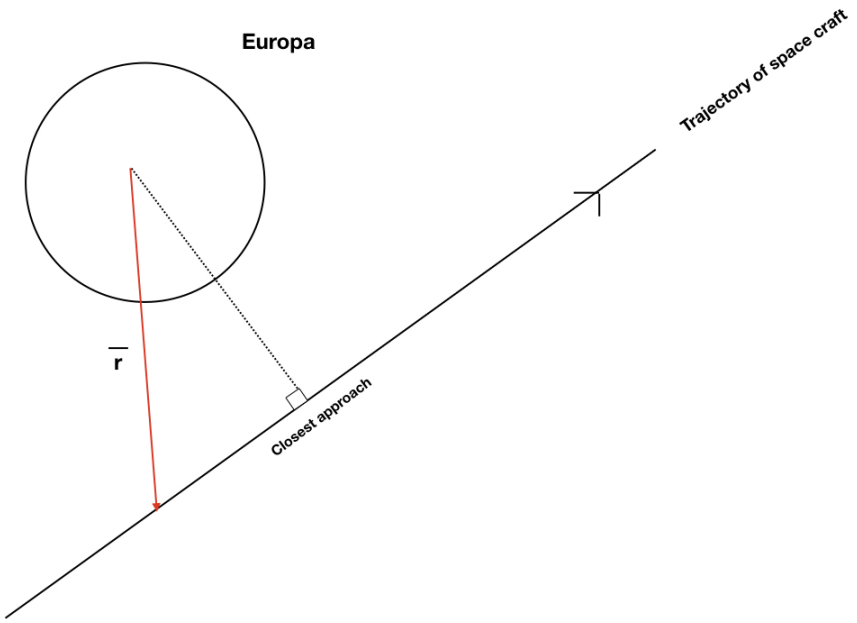

Figure 4: The figure illustrates the trajectory of a fly-by from a spacecraft close to Europa. The position vector is indicted as $\vec{r}$

where C is a constant, **M** is the magnetic moment and **r** is the position vector to where the field should be evaluated.

3 The induction method

The physics behind induction was first described by the scientist Michael Faraday. Electromagnetic induction relies on the fact that a change in magnetic flux will cause an inductive response in a conductor nearby [Purcell and Morin, 2013], i.e. a changing magnetic field will result in a curl of the electric field (which also can be time-dependent). Therefore, to lay out the overview of induction, we begin by considering Faraday's law:

$$\nabla \times \mathbf{E} = -\frac{\partial \mathbf{B}}{\partial t} \tag{2}$$

Faraday's law reveals the mechanism behind electric induction. From equation 2, we see that a change in time in the magnetic field will result in an induced electric field in a conductive material. Or rather, a time change in the magnetic field corresponds to an induced electric field. The induced field will be generated by **eddy currents** inside the material, currents which in turn reduce the background field inside the conductor. The effect of the eddy currents on the magnetic field is shown in figure 5. This means that in the case of a conductor, the total magnetic field will avoid the body itself and "go around" it. The induced field is of high importance since it stores information about the conductive body, such as its **conductivity**, **structure** and **size** [Khurana et al., 2009].

3.1 A time-varying magnetic field

To describe the system of Jupiter and its moons, we turn use the physics behind **electromagnetic induction** and a time-varying magnetic field. In fact, Jupiter's magnetic dipole axis is tilted with respect to its rotation axis. The Galilean moons travel in the equatorial plane (also called the jovigraphic equatorial plane) of the planet, and will thereby experience a time-varying magnetic field as they orbit the planet. The field changes periodically with the rotation frequency of Jupiter (also called the synodic frequency). To be able to measure the magnetic field close to a moon, we have to do in-situ measurements. To do so, we send probes to measure the field for us. This method would be difficult to use if no angle was present between the rotation xis and the magnetic dipole moment axis, since the precision of the instruments would have to be much higher. Therefore, other methods are more effective to detect such small changes with time.

This variation results in induced electric currents inside the moons if a conductive material with sufficient electrical conductivity is present. Physically, this means that if a spacecraft travels past the moon, it would measure a different magnetic field than predicted, since with no moon present the induced field will superpose with the background field (also called primary field or jovian field). The currents from the plasma around the moon will also superpose with the background field, however, this effect will be discussed qualitatively but not taken into account in the model.

Both Khurana et al. [1998b] and Kivelson et al. [1999] have shown evidence for the existence of sub-surface oceans on both Europa and Callisto, by showing that the dominant large-scale features of the magnetic field perturbations are consistent with induced magnetic dipoles, using data from the Galileo spacecraft's flybys. In these models, the moons are assumed to be perfectly conducting spheres, i.e. they are assumed to have a conducting layer close to the surface uniformly across their bodies- a vital assumption. Similar results have been shown for Europa by Kuramoto et al. [1998].

Now, if induction is present, this could be evidence of the existence of a conductive medium such as an ocean, metals, silicates, or an ionosphere. To investigate the induction in the moons, Jupiter can be modeled as a **dipole field** and the moons are assumed to possess layers with the properties of a **perfect conductor**. From equation 2, it is clear that the induced magnetic field will oppose the direction of the inducing field, but be of the same magnitude [Kivelson et al., 2000]. This study aims to begin by modeling the magnetic field of Jupiter and the inductive response from Europa, and validate the model using Galileo data and previous models by Khurana et al. [2009].

The measured magnetic field can reveal important information about the conductor itself, i.e. the moon in this case. From the field, one can for instance find the size and shape of the conductor, as well as the conductivity of the inductive medium. Theoretically, if the moon is assumed to be a perfect conductor, a change in the magnetic field strength with time leads to eddy currents inside the conductor. And in turn, these eddy currents lead to a secondary field around the moon, shown in figure 5. The induced field (the secondary field) will reduce the primary field inside the conductor.

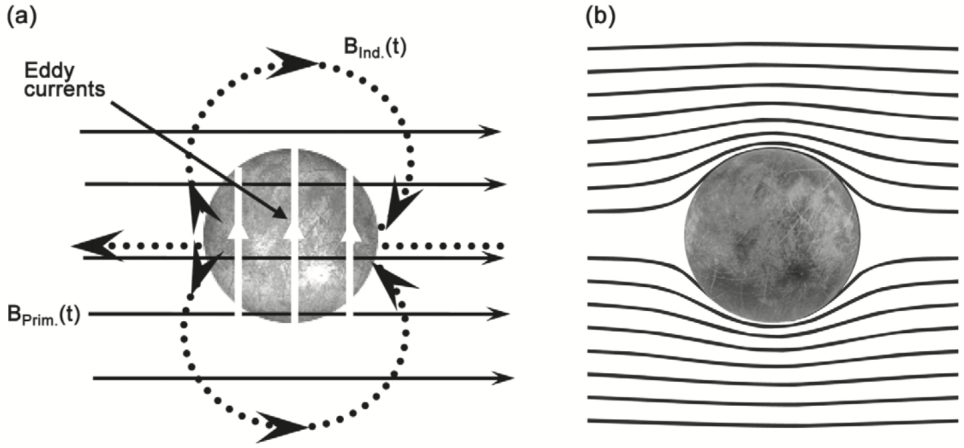

Figure 5: A time-varying primary field is shown in (a), as solid black lines. This field generates eddy currents (white arrows) inside the moon. The eddy currents, do in turn, induce a field shown by the dotted lines. In (b) the total field is shown, as the primary and induced field combine to a time-varying field that surrounds the conductor (Figure 2 from the paper Khurana et al. [2009]

Furthermore, the induced field can be described using **Ampere's law** [Khurana et al., 2009]:

$$\nabla \times \mathbf{B} = \mu_0 \mathbf{J} + \mu_0 \epsilon_0 \frac{\partial \mathbf{E}}{\partial t} \tag{3}$$

where $\mathbf{J}$ is the electric current density, $\mu_0$is the magnetic permeability of free space and ϵ_0 is the permittivity of free space. Now we want to consider Ohm's law [Khurana et al., 2009]:

$$\mathbf{J} = \sigma[\mathbf{E} + \mathbf{v} \times \mathbf{B}] \tag{4}$$

where $\mathbf{v}$ is the flow velocity and σ is the conductivity of the material which is induced. Using equation 2, 3 and 4, **the electrodynamic equation** can be derived [Khurana et al., 2009]:

$$\nabla^2 \mathbf{B} = \sigma \mu_0 [\frac{\partial \mathbf{B}}{\partial t} - \nabla \times (\mathbf{v} \times \mathbf{B})] \tag{5}$$

The electrodynamic equation is crucial to describe the magnetic field around Jupiter- but it can be simplified. Assuming no spatial variations in the conductivity of the conductor and no convection in the moons, equation 5 simplifies to the diffusion equation [Khurana et al., 2009]:

$$\nabla^2 \mathbf{B} = \mu_0 \sigma \frac{\partial \mathbf{B}}{\partial t} \tag{6}$$

And this equation can be solved to describe the field around the planet and the moons.

3.2 The induced magnetic field from a uniformly conducting shell

To model the induced magnetic field from a uniform conductor, the system shown in figure 6 is considered. This model illustrates an insulated core surrounded by a shell of uniform conductivity σ. And where the shell has inner radius r_1 and outer radius $r_0 = r_1 + h$, Moreover, the core has inner radius r_0 and outer radius $r_m = r_0 + d$ (note that the radius of the moon is r_m). Using this model, the depth, thickness, and conductivity can be constrained in an elementary and effective way.

Now, one can turn to the classical electromagnetic problem of a **time-varying magnetic field** and how the response will look in the case of the model in figure 6. And from such a model, the inductive response of a uniform conducting sphere can be described [Zimmer et al., 2000].

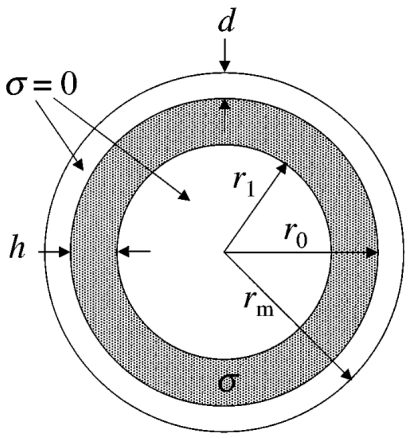

Figure 6: The figure illustrates the assumed spherical shell model for the moons and their conductive layer. Figure adapted from figure 1 in the paper by Zimmer et al. [2000].

3.3 Equations for the magnetic field model

Furthermore, the electromagnetic theory allows us to describe the magnetic field induced by a uniform conducting shell, as done in the previous section, which results in equation 6. Note that the permeability is assumed to be the permeability in a vacuum, μ_0, everywhere (inside and outside the conducting shell). Hence, in the insulating layer of the moon the following must hold:

$$\nabla^2 \mathbf{B} = 0 \tag{7}$$

Also, note that the equation holds outside the conductive shell assuming the conductivity to be small as well as the flow velocity to be zero. It is important to note that the solution to the diffusion equation ignores the plasma outside the conductor, as well as the displacement current is assumed to be negligible in equation 6 and 7. Now, the background field from Jupiter can be modeled in polar coordinates as [Neubauer, 1999]:

$$\begin{aligned} B_r &= 2B_{eq}\sin(\alpha)L^{-3}\cos(\Omega t) \\ B_\theta &= B_{eq}\cos(\alpha)L^{-3} \\ B_\phi &= -B_{eq}\sin(\alpha)L^{-3}\sin(\Omega t) \end{aligned} \tag{8}$$

where L is the Jovian radius, α is the inclination angle between the magnetic dipole axis and the rotation axis of Jupiter, and B_{eq} is the magnetic field strength from Jupiter at the equator plane.

3.4 Total magnetic field

In addition, since the solutions always are a superposition of linearly polarized fields, the following conditions must be fulfilled for the total time-varying field:

(i) the magnetic field, **B**, must be continuous across the boundaries of the shells (implied by the fact that the permeability, μ_0, is uniform)

(ii) the magnetic field, **B**, cannot be infinite at $\mathbf{r} = 0$, i.e. the field must be defined at the center of the sphere

(iii) far away from the sphere, the magnetic field, **B**, has to be asymptotically equal to B_{prim} (the external field)

Using the assumption of linear superposition, the total field is given by:

$$\mathbf{B}_{tot} = \mathbf{B}_{background} + \mathbf{B}_{induced} \tag{9}$$

where the induced field (also called secondary field) is denoted by $\mathbf{B}_{induced}$. The induced field will be in the form of a dipole field since the primary field is assumed to be uniform and the conductivity distribution is spherical. The total field will "avoid" the conductor (moon), as shown in figure 5. Moreover, the induced field is given by the expression for a dipole field given in equation 1, and will for this case be expressed as follows:

$$\mathbf{B}_{induced} = \frac{\mu_0}{4\pi}[(\mathbf{r}\cdot\mathbf{M}) - r^2\mathbf{M}]/r^5 \tag{10}$$

where the moment, $\mathbf{M}$, has the same frequency, ω, along $\mathbf{e}_0$, in accordance with the background field. Therefore, the moment is given by the following expression:

$$\mathbf{M} = -\frac{4\pi}{\mu_0}Ae^{i\phi}\mathbf{B}_{background}\frac{r_m^3}{2} \tag{11}$$

Note that the background field can be estimated using a polynomial fit of the data (see discussion in section 3.6), while the induced field at the location of the spacecraft is modeled using equation 10. Hence, the induced field is modeled using the primary field which results in a theoretical magnetic moment.

Now equation 10 can be written in the following way [Zimmer et al., 2000]:

$$\mathbf{B}_{sec} = -Ae^{-i(\omega t-\phi)}B_{prim}[3(\mathbf{r}\cdot\mathbf{e}_0)\mathbf{r} - r^2\mathbf{e}_0]\frac{r_m^2}{2r^5} \tag{12}$$

where ϕ, and the wave-vector $\mathbf{k}$, in equation 12 are given by [Parkinson, 1983]:

$$\begin{aligned} Ae^{i\phi} &= (\frac{r_0}{r_m})^3\frac{J_{5/2}(r_0k) - J_{-5/2}(r_0.k)}{J_{1/2}(r_0k) - J_{-1/2}(r_0k)} \\ R &= \frac{r_1kJ_{5/2}(r_1k}{3J_{3/2}(r_1k) - r_1kJ_{1/2}(r_1k)} \\ k &= (1-i)\sqrt{\mu_0\sigma\omega/2} \end{aligned} \tag{13}$$

where k is a complex wave vector, J_m is the Bessel function of the first kind and order m, and r_0, r_1 and r_m are given as above. Note that the physical field that can be measured is given by the real part of equation 12. From this, we can see that A is the normalized amplitude and ϕ is the phase lag, of the induced dipole moment relative to the primary field. The maximum intensity of the equatorial induced field is reached when $B_{seq,eq} = AB_{prim}/2$, which occurs one time each period ($P = \frac{2\pi}{\omega}$).

3.5 Magnetic field equations in frequency domain

The primary field can be written in the frequency domain by assuming that the field oscillates with frequency ω along $\mathbf{e}_0$ (the unit vector), and can be written in a complex form as:

$$\mathbf{B}_{bakground} = B_{bakground}e^{-i\omega t}\mathbf{e}_0 \tag{14}$$

where $\mathbf{B}_{background}$ is the primary field with the direction defined by the unit vector $\mathbf{e}_0$. Thereby, the real part of equation 14 corresponds to the measurable background field. However, the field is neither constrained to necessarily oscillate with the frequency ω nor to oscillate in a single direction, but one can express the linear solutions of equations 6 and 7 as a superposition (which as well is linear).

3.6 Skin depth and conductivity

The primary field given in equation 14 can be expressed in terms of skin depth:

$$B = B_{prim} e^{-z/s} e^{-i(t-z/s)} \tag{15}$$

The skin depth in equation 15 describes how the signal decays in a medium by e-folding, and is given by:

$$s = \frac{1}{\sqrt{\mu_0 \sigma \omega / 2}} \tag{16}$$

It is worth realizing that the wave vector, k, in equation 13 can be expressed in terms of skin depth, s.

From equation 16, it can be seen that for a medium with high conductivity (alternatively if the signal has a high frequency), the skin depth is expected to be small. It is also worth noting the case when the skin depth is larger than the thickness of the object since then the signal cannot significantly penetrate the material.

Jupiter has a spin period of about 10 h, which corresponds to a skin depth of 30 km in a medium with the conductivity of 10 S/m. If the moon has a thickness that is larger than the skin depth, the wave will be reflected back, creating an induced field that amplifies the primary field outside the conductor.

It is of interest to investigate the conductive sheet with a conductivity close to one of Earth's oceans, i.e. 2.75 [S/m] [Khurana et al., 2009]. From the table in the paper by Khurana et al. [2009] the conductivity of common geophysical materials is listed. From the table it is clear that the induction measured by the Galileo spacecraft cannot be explained by the presence of pure water, rocks etc. since the skin-depths of such materials are much larger than the dimensions of the moons. As well as pure water has an almost non-existent conductivity. Materials such as copper or iron could be behind the induction but are unlikely to be found on the moons. Therefore, as argued by Khurana et al. [2009], a salty sub-surface ocean is the most probable cause of the induction measured. Further, it is believed that, for instance, Ganymede probably has a metal core (similar to Earth) and Europa consists of silicate materials.

3.7 The trajectory of the spacecraft

To define the coordinate system of the magnetic field, one must consider the trajectory of the spacecraft relative to the motion of the moon. In figure 7, flyby E4 is shown relative to Europa.

3.8 Determination of closest approach

To be able to compare the data with the model, we choose a time-interval small enough so that the longitude of the spacecraft relative to Jupiter does not change significantly. To find this interval, it is useful to consider the closest approach of the spacecraft and then choose a time before and after, to model. This can be done by plotting the length of the position vector against time and extracting the time for the minimum. Such a plot is shown for the E4 flyby in figure 8.

3.9 Estimation of the Jovian background field at the space craft

To estimate the background field (also called the Jovian background field) from Jupiter at the location of the spacecraft, we can do a polynomial fit of the data since the background field is small far away from the inducing dipole (Jupiter in this case). To do this, one can plot the data and filter out the induction part, and make a polynomial fit for the data before and after the closest approach of the spacecraft. This can for example be done using Matlabs built-in function **polyfit** The filter for flyby E4 is shown in figure 9. This field is then added to the modeled induced field using equation 9.

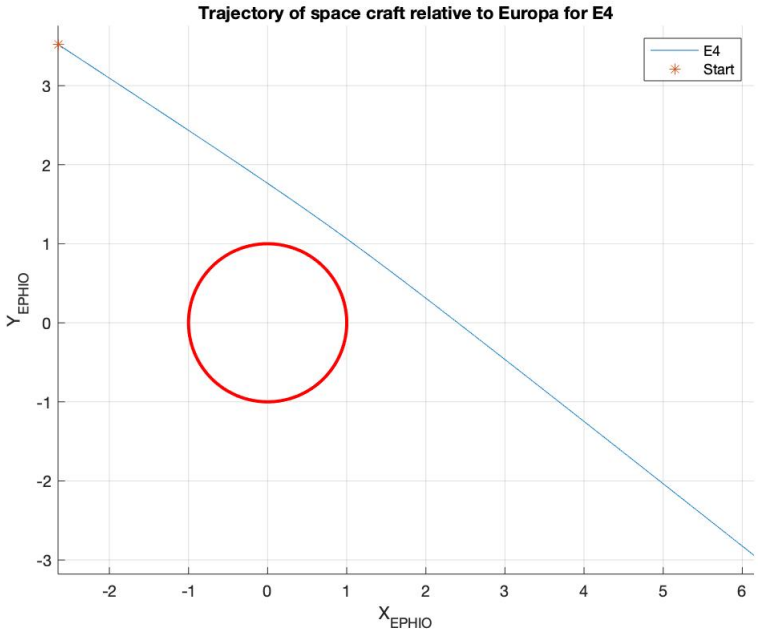

Figure 7: The trajectory of the E4 flyby, where the path of the spacecraft is shown relative to Europa (centered at (0,0)).

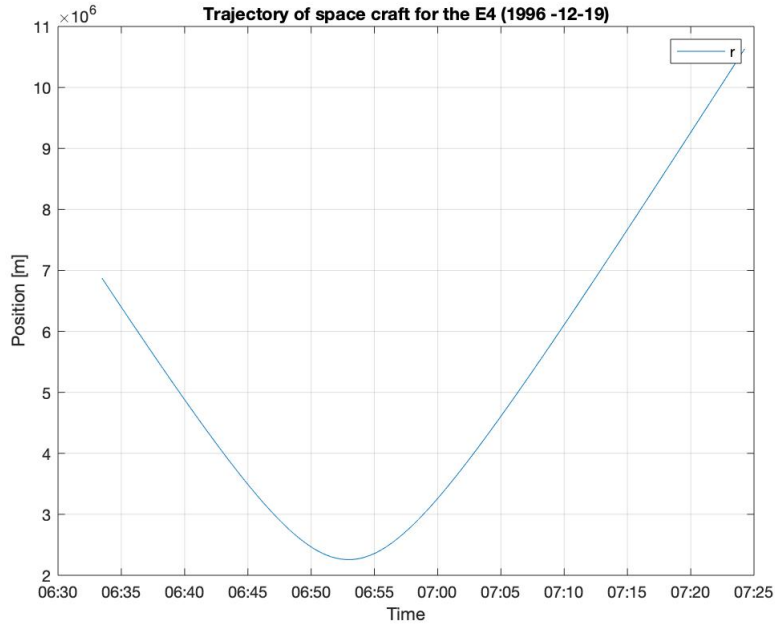

Figure 8: The length of the space crafts position vector for the E4 flyby is plotted against time to determine the closest approach, which occurred when the function has its minimum value.

3.10 Magnetic field strength depending on the conductivity and shell thickness

To investigate the source of the induction further, we can investigate what happens to the induced field when the conductivity of the sheet is changed. This can be done by considering equation 13, by varying the conductivity (σ).

Additionally, as seen in equation 13, the induced field also depends on the depth of the conductive

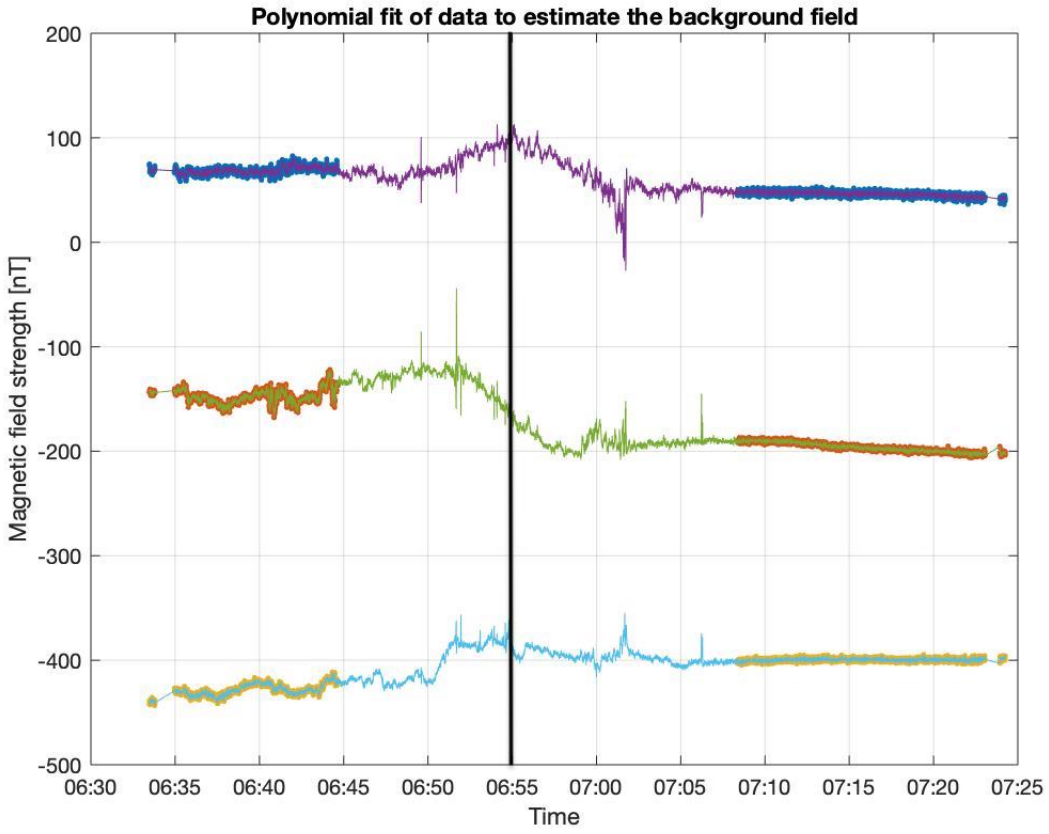

Figure 9: To estimate the Jovian background field, the data can be filtered and a polynomial fit can be used to estimate the background magnetic field, in this case, for flyby E4. The data extracted for the filter is highlighted.The closest approach is indicated with a black line.

layer, and it is therefore interesting to investigate the field for different thicknesses (h). Both σ and h are difficult to constrain since the nature of the conductive sheet is unknown, and further discussion is needed.

4 Analysis and results

4.1 Definition variables

In table 2, the variables used to model both the background magnetic field from Jupiter and the induced field at the location of the spacecraft, are listed. The conductivity, σ and the thickness of the conductive layer, h, are changed and investigated in a later section since they most likely vary in reality.

Table 2: In the table, the different variables needed to calculate the magnetic field at Europa are listed. Values extracted from Nordling and Österman [2020].

Variable	Name	Value
L	Distance to Jupiter in units of Jovian radius (r/R_j)	9.5
P	Synodic period [h]	11.1
h	thickness of conductive layer [m]	100 $\times 10^3$
d	thickness of the surface ice [m]	50 $\times 10^3$
r_m	radius of the moon [m]	1560 $\times 10^3$
r_0	distance to insulating layer [m]	$\mathrm{r}_m - d$
r_1	distance to conductive layer [m]	$\mathrm{r}_m - d - h$
μ_0	permeability of free space [mkgs$^{-2}A^{-2}$]	1.2566 $\times 10^{-6}$
σ	conductivity of salty [sm^{-1}]	2.27

4.2 Data extraction and management

To validate the model presented in this study, data collected by the Galileo probe in the 1990s is used. In this section, data extraction and management are presented. In the dataset, the different flybys are listed in both Jupiter Sys-III and EPHIO coordinates, see table 3 for the outline. From the data, it is possible to extract magnetic field strength in both EPHIO and Jupiter System-III coordinates, with corresponding location, longitude, and time from the spacecraft.

The data was extracted from the following webpage:Galileo data

Table 3: In the table, the form the data is stored in is shown, in both EPHIO and Jupiter System-III coordinates. The magnetic field data is divided into the direction of r, θ and ϕ for the EPHIO-system coordinates and in the direction of x, y and z direction for the Jupiter system III coordinates. For the definition of the two coordinate systems, see table 3.

System								
EPHIO	time	B_r	B_θ	B_ϕ	B [nT]	R[R_E]	Lat[deg]	$\mathrm{E}_{Long}[deg](W_{long}[deg]$
JUPITER SYS-III	time	B_x	B_y	B_z	B [nT]	X_{RE}	Y_{RE}	Z_{RE}

4.3 Trajectories of the spacecraft relative to Europa

To model the induced magnetic field at the location of the spacecraft, it is useful to consider the different flybys in relation to each other, which is done in figure 10. In the figure, all investigated trajectories are illustrated, with the distance shown in Europa radii.

As seen in the figure, the flybys occurred at different locations relative to the moon, where for instance the E11 occurred close to the north pole while E19 was closer to the equator of the moon. Depending on the trajectory of the spacecraft, the induced magnetic dipole moment will be observed in different components of the measured magnetic field. in different directions, as illustrated in figure 10.

4.4 The time-varying field for a synodic period

To get an intuition for how the magnetic field from Jupiter. looks like at Europa, it is of interest to plot the time-varying field for a synodic period, as shown in figure 11. In the figure, the primary

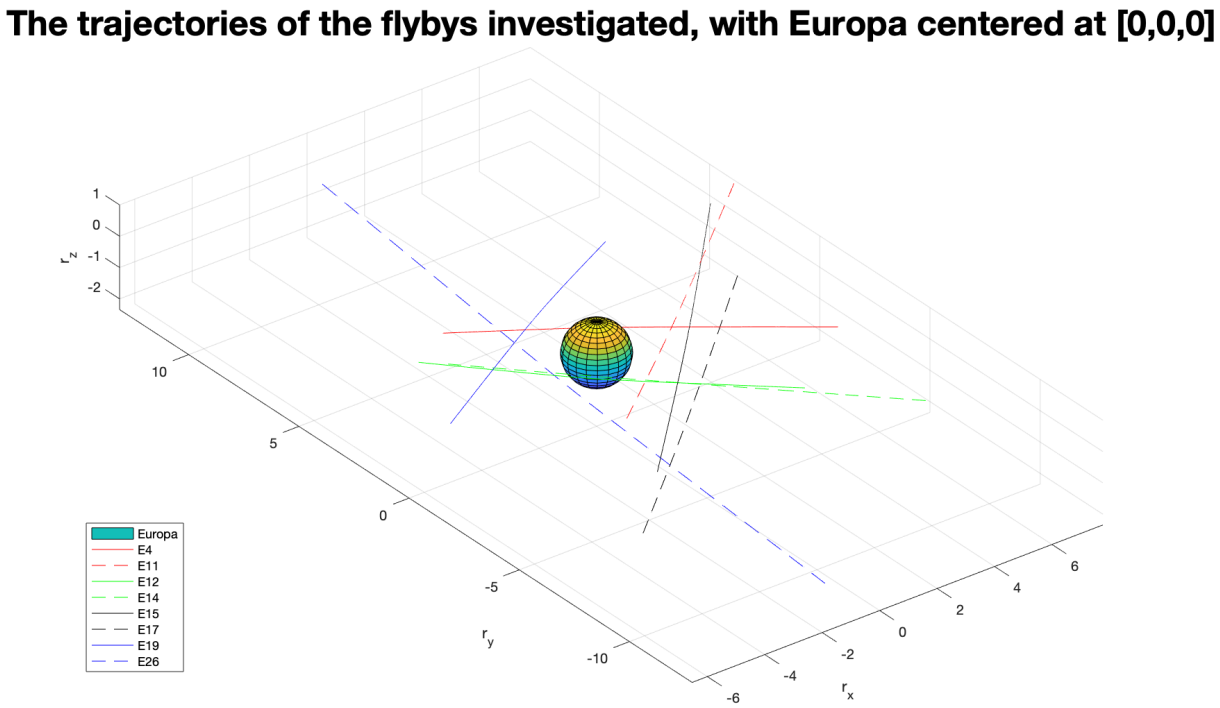

Figure 10: All investigated trajectories are shown relative to Europa, in Cartesian coordinates. The trajectories are straight lines since only a short period of time is illustrated for each flyby. The moon, Europa, is centered at (0,0,0). The axes are scaled to Europa radii.

field and the secondary field are plotted. As expected, the field varies sinusoidally in the x and y-direction, while the field is constant in z-direction. Furthermore, the induced field is in the opposite direction, with a smaller amplitude compared to the primary field, in accordance with the theory.

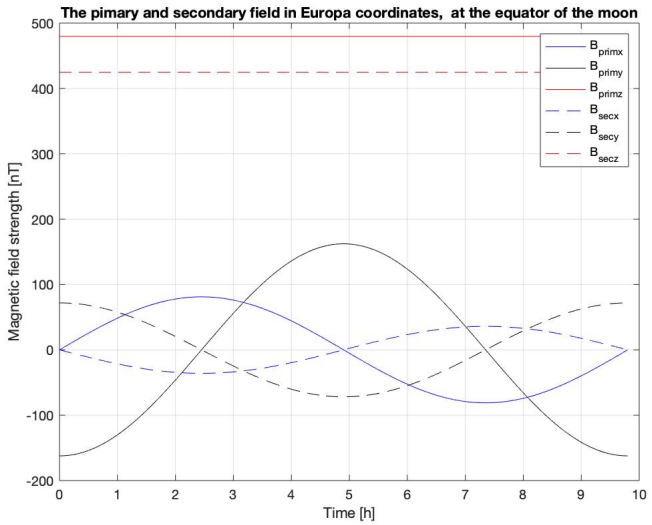

Figure 11: The theoretical primary and secondary field are plotted in EPHIO coordinates, at the equator of the moon, plotted for a whole synodic period of Jupiter (11.1 h).

4.5 Interaction with plasma

In this thesis, corrections due to plasma currents are not taken. However, it is of interest to discuss the impact of plasma currents in a qualitative way for the analysis of the model and comparison with the data. In general, the flow velocity of the plasma will be greater than the Kepler velocity of the moon, resulting in plasma currents around the moon as it orbits the planet. In figure 12, it can be seen that the magnetic field strength actually varies during a synodic period, a variation that can be explained by plasma currents. There are two main reasons for these abnormalities (seen as spikes in the data); **Ionosphere currents** and **plumes** (which may lead to an outburst of plasma) can cause discrepancies in the data.

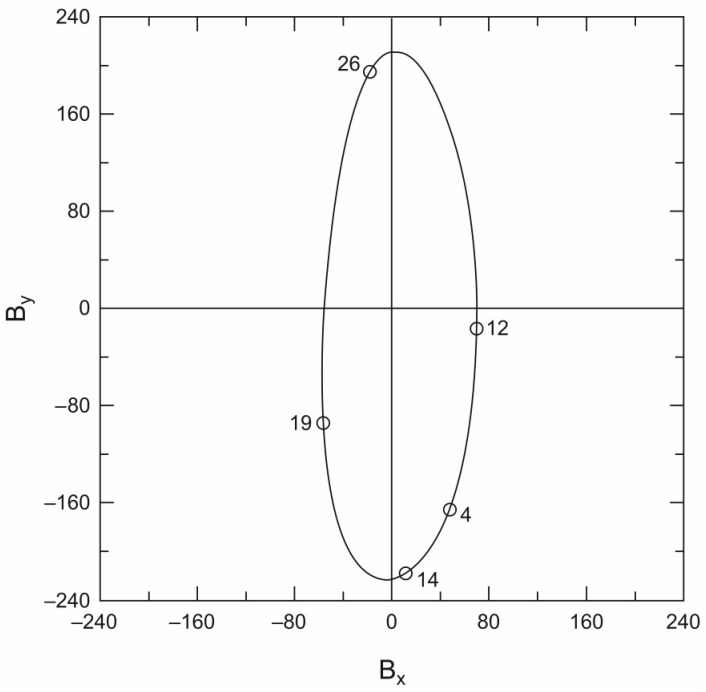

Figure 12: The figure shows Jovian magnetic field i the x and y direction, for Europa, during one synodic period of Jupiter. In the figure, four flybys are indicated. The figure is from Zimmer et al. [2000], figure 5.

4.6 The modeled magnetic field

From the background field (primary field), the induced field (secondary field) at the location of the spacecraft can be modeled. In equation 11, the position vector is defined as the position of the spacecraft, which can be extracted from the data (in EPHIO coordinates).

Then, by using equation 14, the magnetic field at the location of Europa can be calculated. This field can thereby be used to calculate the expected induced field using equation 10, where the induced field is calculated at the location of the spacecraft.

Furthermore, to find the total field, the Jovian background field is estimated using a linear fit of the data. The total field, the background field, and the induced field are shown in figure 13 and 14, together with data from the Galileo space probe. The modelled field for flybys E11, E12, E14, E15 and E19 are shown in **Appendix 7.1**.

In figure 13 and 14 it can be seen that the modeled field corresponds fairly well with the measured field by the Galileo spacecraft. The background field (straight lines in both figures) follows the gradient of the data, and the model of the primary field is, hence, consistent with the data. Moreover, the modeled induced field follows the shape of the data, with no induction in the z-direction, as expected. The background field estimation (primary field), is arguably more precise than the one made previously by Khurana et al. [1998a] since the background field is estimated from the data,

rather than using the theoretical field.

Furthermore, spikes can be seen in all collected data, for instance in figure 13, at around 00:08. These abnormalities can be a result of currents in the ionosphere. The spikes seen in flyby E12 and E24 could also be explained by the presence of plumes [Jia et al., 2018]. In addition, the violent disturbances shown in for instance figure 18 could be explained by Alven wings and plasma fluctuations.

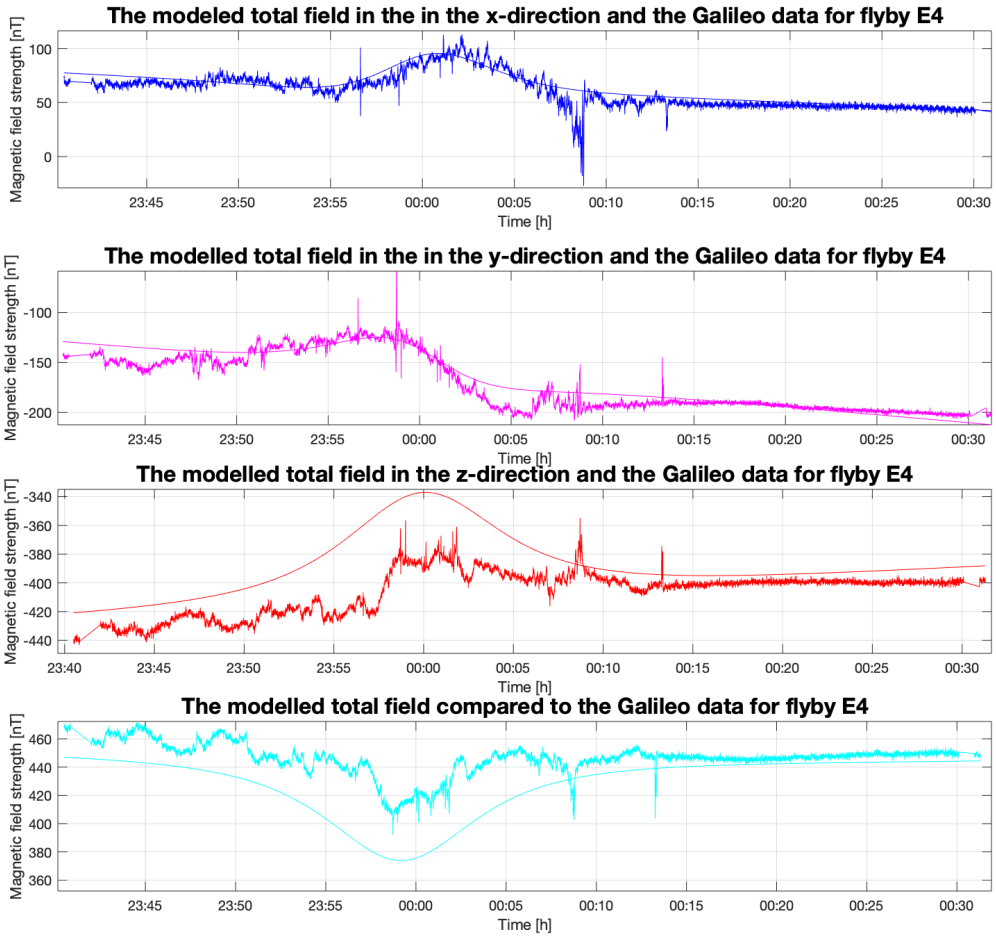

Figure 13: The total magnetic field is calculated using the model. The total field (background and induced field) is presented in each direction (EPHIO coordinates) for the E4 flyby. as well as the total field) for the E4 flyby. The sum of the components ($\vec{\mathbf{B}}$) is also shown. The model is also compared to the corresponding Galileo-data.

The model for the primary field agrees well with the data in all cases, however, this is not the case for the induced field. For flyby E4 and E14, figure 13 and 14 respectively, the induced field matches well with the expectation. But in the case of E11, E12, E15 and E26, see appendix 7.1, the induced field matches quite well with the data in the x and y direction, but not in the z-direction (and consequently the sum does not match). Additionally, by considering figure 22 in appendix A, there seems to be a poor match between the data and the modeled field in all directions except in the y-direction.

4.7 The inductive response depending on the conductivity

The conductivity of the conducting sheet is not known, and it is therefore of interest to investigate how the induced field changes with the conductivity of the sheet. The conductivity will change the amplitude, A, which follows from equation 13.

The magnetic field strength (in EPHIO coordinates) for different conductivity's is shown in figure 15. The modelled induction is compared to data from the Galileo space craft. From the figure it is

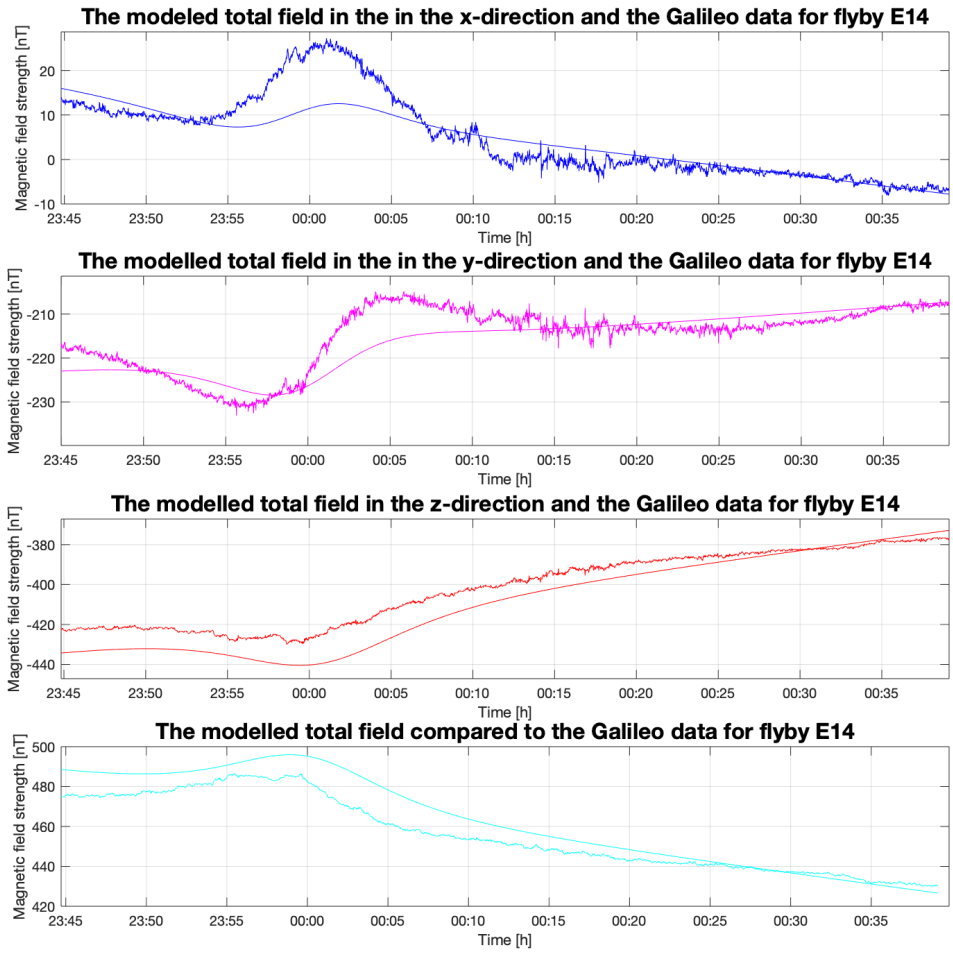

Figure 14: The total magnetic field is calculated using the model. The total field (background and induced field) is presented in each direction (EPHIO coordinates) for the E4 flyby. as well as the total field) for the E14 flyby. The sum of the components (B) is also shown. The model is also compared to the corresponding Galileo-data.

clear that a low conductivity (ocean water = 2.75 S/m) gives the most accurate model representation of the induction. Therefore, it seems most likely that the moon possesses a sub-surface ocean rather than containing metals and such.

4.8 The inductive response depending on the thickness of the conductive layer

The strength of the induced field depends on the thickness of the conductive layer, as seen in equation 13. Thereby, it is of interest to investigate how the induction changes with increasing thickness, h. How the induction depends on the shell thickness is shown in figure 16. From the plot it is obvious that the thicker the conductive layer, the larger is the induced field, as expected. Although it is difficult to precisely say which thickness corresponds to the most accurate, the assumption of the thickness to be around 100 km thick seems reasonable from plot 16.

4.9 Constraints of the amplitude (A) and phase lag (ϕ)

Using equation 10, one can model the induced magnetic field from a time-varying primary field. The primary field of Jupiter is described by equation 14. To find the inductive response, the magnetic dipole moment, M, is considered, given by equation 11.

First, let us consider the case of an **ideal conductor**, where the moon is assumed posses a uniformly

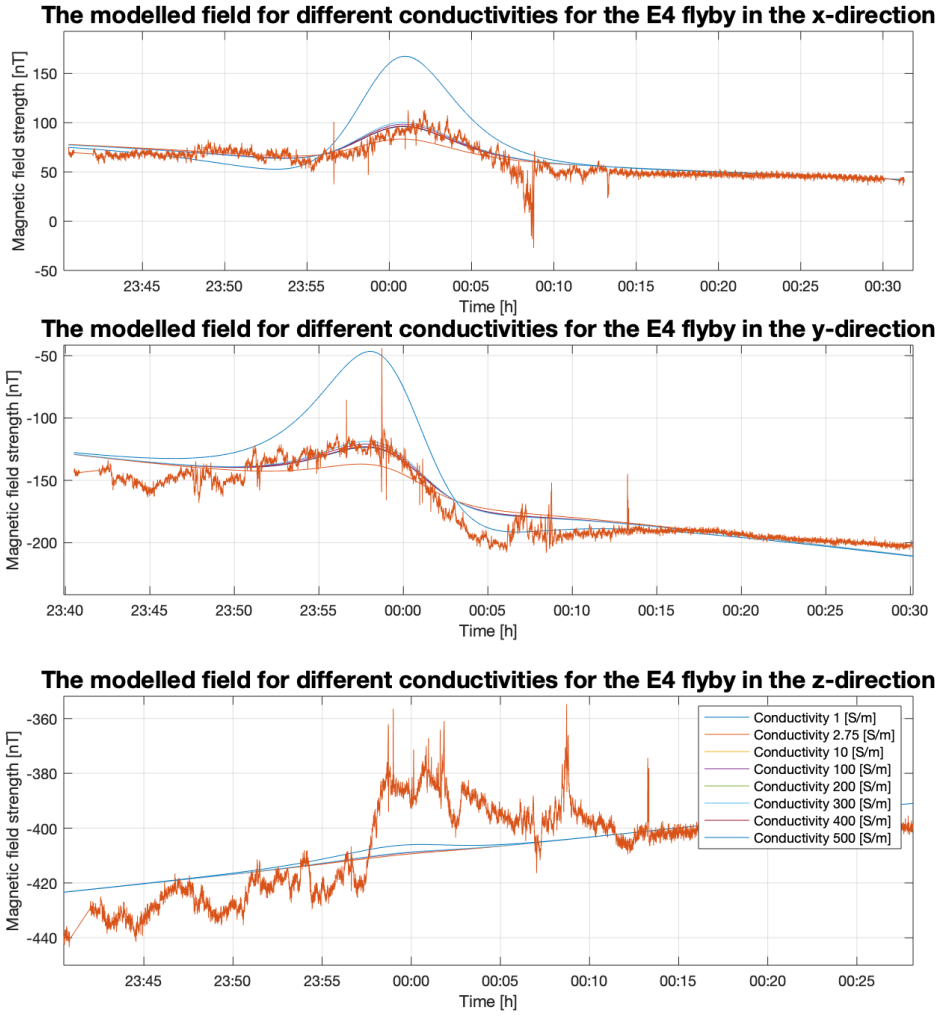

Figure 15: The induced field depending on the conductivity of the conductive layer.

conducting shell. Then the induced field will be generated instantaneously, i.e. the phase lag $\phi = 0$ between the primary and secondary field is zero. Therefore, we can define A using equation 13, with $\phi = 0$. The model shown in figure 6 illustrates the simplest model to constrain the thickness, conductivity and depth of the conducting shell. Furthermore, the induced field is given by the real part of equation 10, hence, the physical field can be written as (taking phase into account):

$$\mathbf{B}_{sec}(t) = A\mathbf{B}_{sec,\infty}(t - \frac{\phi}{\omega}) \tag{17}$$

where $B_{sec}(t)$ is the instantaneous induced field by a spherical shell at time t. This field is equivalent to the field created at the time shifted by a factor depending on the phase, $A(t - \frac{\phi}{\omega})$. Now, we want to constrain ϕ and A. If the conductivity is finite, i.e. $\sigma < \infty$, then it is possible to show that the following must hold:

$$\begin{aligned} 0 \leqslant & A < (\frac{r_0}{r_m})^3 \\ 0^\circ < & \phi \leqslant 90^\circ \end{aligned} \tag{18}$$

i.e. the induced field will always be created at a time after the primary field, shifted with a phase ϕ, and the amplitude will always be smaller than that of a perfect conductor- which physically makes sense [Zimmer et al., 2000].

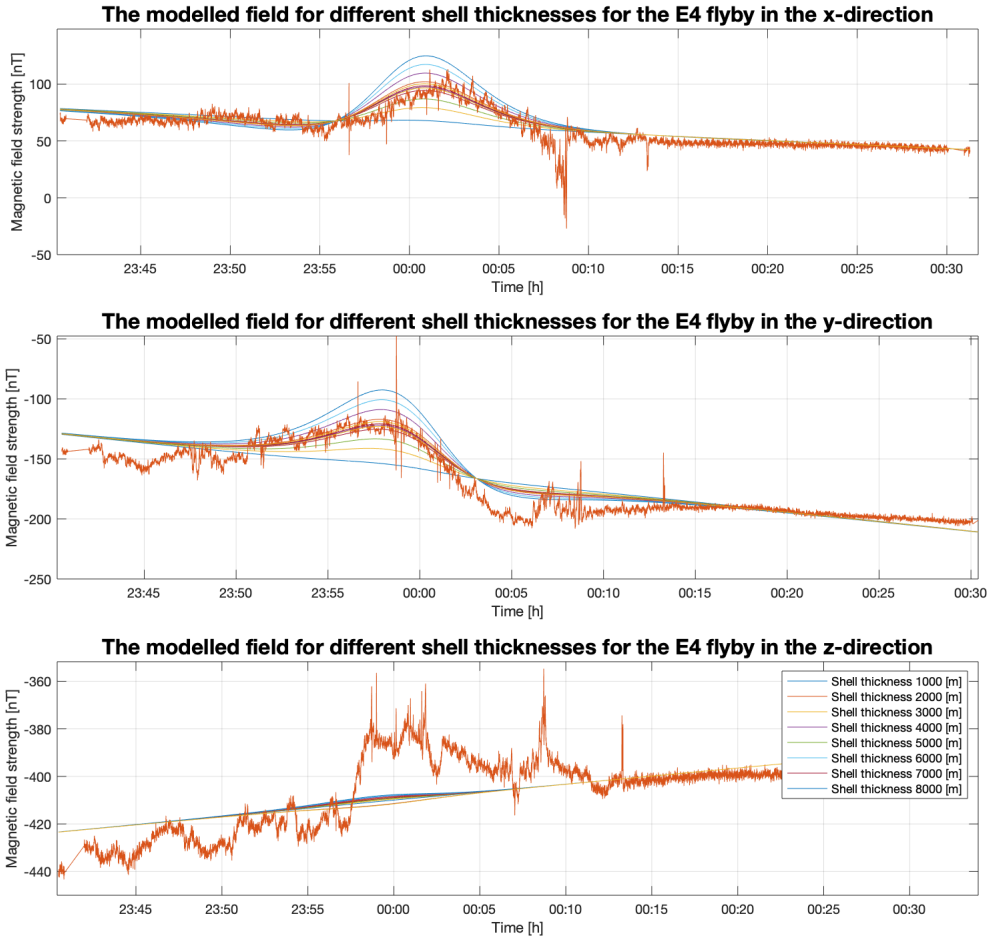

Figure 16: The induced field depending on the shell thickness, h, of the conductive layer. The data used originates from the E4 flyby.

Furthermore, A will vanish if the conductivity of the shell is low, as well as if the conductor is far from the surface. I.e, A will vanish if the following holds:

$$\begin{aligned} \sigma &\ll \sigma_m \\ r_o &\ll r_m \end{aligned} \tag{19}$$

Let us consider a few different cases. The paper by Zimmer et al. [2000], considers the cases:

Highly conductive shell: This case is defined as $\sigma \gg \sigma_m$ must hold and the inductive response will be almost ideal (as the response for a perfect conductor). Therefore, one can consider the limit when $A \to 1$ and $\phi \to 0$.

Slightly conductive shell: This case is defined as $\sigma < 0.1\sigma_m$ must hold and therefore, the inductive response will be small, similar to the response from a perfect insulator. Then A and ϕ will be constrained as $0 \leq A < 0.02$ and $88° < \phi \leq 90°$.

It is worth noting that the ideal case, where the amplitude takes its maximum value and the phase its smallest value, can as well occur for an intermediate shell thickness, which is not to be expected. Also note that if the moon is large enough, then the shell can be smaller than the skin depth, which contradicts theory [Zimmer et al., 2000]. In figure 17, the magnetic field in each direction is plotted for several amplitude factors, A.

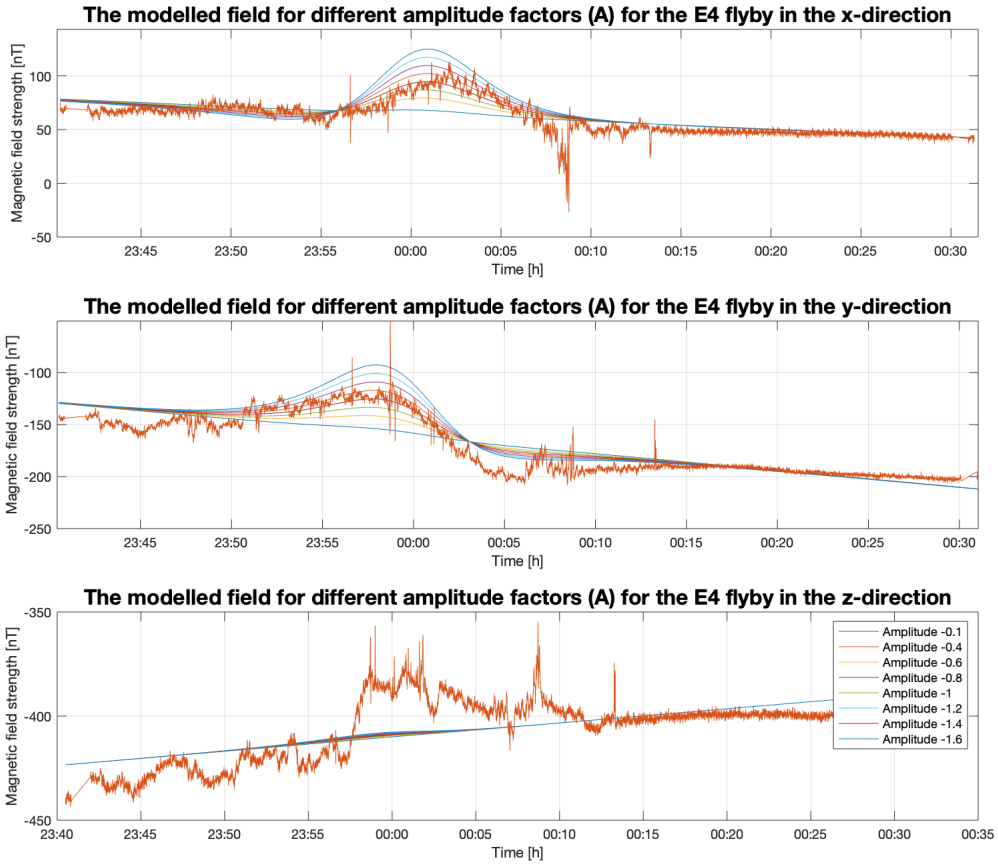

Figure 17: The amplitude factor, A, is changed to investigate how the induced field changes depending on the amplitude factor. The data for the E4 flyby is also plotted, to allow comparison between the model and the data, with the aim to determine which A corresponds to the real case.

4.10 The influence of a conductive core/mantel or ionosphere

In the model presented in this study, the material surrounding the ocean layer is assumed to be insulating. However, in a similar discussion which is presented by Kivelson et al. [2000], this does not necessarily have to be the case. Kivelson et al. [2000] for instance, discusses the possibility of the material being conducting, for example, by consisting of a silicate mantle or a silicate core. Moreover, the induction could be explained by the presence of an ionosphere.

The model presented in this study is built around the assumption that the moon can be viewed as a perfect conductor since the phase lag is assumed to be zero. And even if the moon had a metallic core (similar to Earth), its small size could never explain the induction measured by the Galileo probe. To get perspective on the sizes we are currently discussing, to achieve an amplitude, A, of 0.5, the core would have to reach from the center all the way up to about 300 km below the surface of Europa, which is not possible considering gravitational constraints [Zimmer et al., 2000].

In contrast, a silicate mantle is not as easy to dismiss. Silicates can be stored in rocks, and while rocks are not conductive, if dissolved in a liquid, the liquid can become very conductive. Although, high temperatures are needed, to make dry rocks very conductive. For instance, several hundreds of degrees Celsius are needed to establish a conductivity of several tens of millister-radians per meter [Zimmer et al., 2000]. Such temperatures are not likely to be reached on an icy moon of Jupiter, since such temperatures inside the moon would case the ice to melt [Kuramoto et al., 1998]. What is also worth noting is the fact that if the ice layer on Europa would melt, it could itself be the cause of the induction, since the melted ice can carry currents, and the underlying mantle, is thereby, shielded from the magnetic background field. In other words, the mantle will not contribute to the

induction no matter its conductivity [Zimmer et al., 2000].

In addition, mineralogical transitions are possible in the mantle of Earth thanks to the pressure from the gravity, but will not be possible on the Galilean moons since they are too small. Kivelson et al. [2000] also discusses the depth of the conductive sheet. As shown in figure 16, a larger shell thickness implies a layer of higher conductivity. Further, another possible explanation for the induction could be the existence of an ionosphere. In this case, the conductive body will be larger than the actual moon, resulting in induced currents closer to the space craft. Moreover, the conductivity is proportional to $\frac{1}{r_0^2}$, implying that the normalized conductivity ($\frac{\sigma}{\sigma_0}$) corresponds to a smaller σ. Hence, a large ionosphere could account for the induction measured [Zimmer et al., 2000].

4.11 Limitations and improvements of the model

It is worth noting that the model is considering an **ideal conductor**, which is not the case in reality. For instance, Khurana et al. [1998a], attempts to fit the data to the model by considering different amplitude factors, A, since A is only 1 for an ideal conductor (or rather the ratio of $(\frac{r_0}{r_m})^3$ for the case of a conductive shell). Unfortunately, it is difficult to constrain A precisely due to the poor resolution of the data, and further investigation is needed to constrain A better. Also, to create a more representative model, the phase lag, ϕ, needs to be considered since, in reality, there will be a time delay between the primary and secondary field. Khurana et al. [1998a] assumes the phase lag, ϕ, to be zero, as in this report, reflecting the ideal case.

Additionally, Kivelson et al. [2000] discusses the accuracy of the model when investigating the E11, E12, E15, E17 and E19 flybys, and comes to the conclusion that the model agrees poorly with the measured magnetic field. In figure 18 this can be seen using the model from this paper, with the largest fluctuations in the z-component. The fluctuations could be explained by plasma currents (with $A \geq A_{ind}$). Further, the difference between the expected and measured field can be a consequence of the position of the moon in the plasma sheet of Jupiter. If the moon is located close to the center of the plasma sheet, the plasma will lead to disturbances due to the presence of Alvén Wings. This was the case for E11, E17 and E19 since Europa was about $1R_E$ from the equatorial plane. For a further discussion on the topic, see Kivelson et al. [2000] since plasma physics is out of the scope of this thesis.

Another limitation is the fact that the nature of the conductive layer is unknown, since characteristics such as the material and the depth the layers have not been able to be determined. With the JUICE-probe, such characteristics can hopefully be constrained further.

To improve the model, corrections for the plasma environment can be taken into account. This has been done by, for instance, Khurana et al. [2009], where it is shown that the value of A does not correspond entirely to the one for a perfect conductor (i.e. $((\frac{r_0}{r_m})^3)$). The model could therefore be improved by constraining A further, considering the fact that the moon is not an ideal conductor in reality. Also, the model has to be adapted to the cases for Ganymede, Io and Callisto, since the three moons have different properties and are located in different plasma environments. In that sense, Europa is the simplest case to model and further discussions have to be made for the other moons.

In addition, **passive low-frequency electromagnetic methods** can be used to investigate the structure of the moons further, perhaps resulting in even better results. Such methods have been used to study, for instance, Earth's own moon, as well as Ceres, which is the largest dwarf planet in the main asteroid belt. One can study the turbulence of the solar-wind to reveal hidden conducting structures. The turbulence gives a broad temporal spectrum for **electromagnetic sounding**. The method utilizes the formation of eddy currents and the magnetic field e-folding property to, using the skin depth, describe the magnetic field in terms of the angular frequency, ω [Grimm et al., 2021].

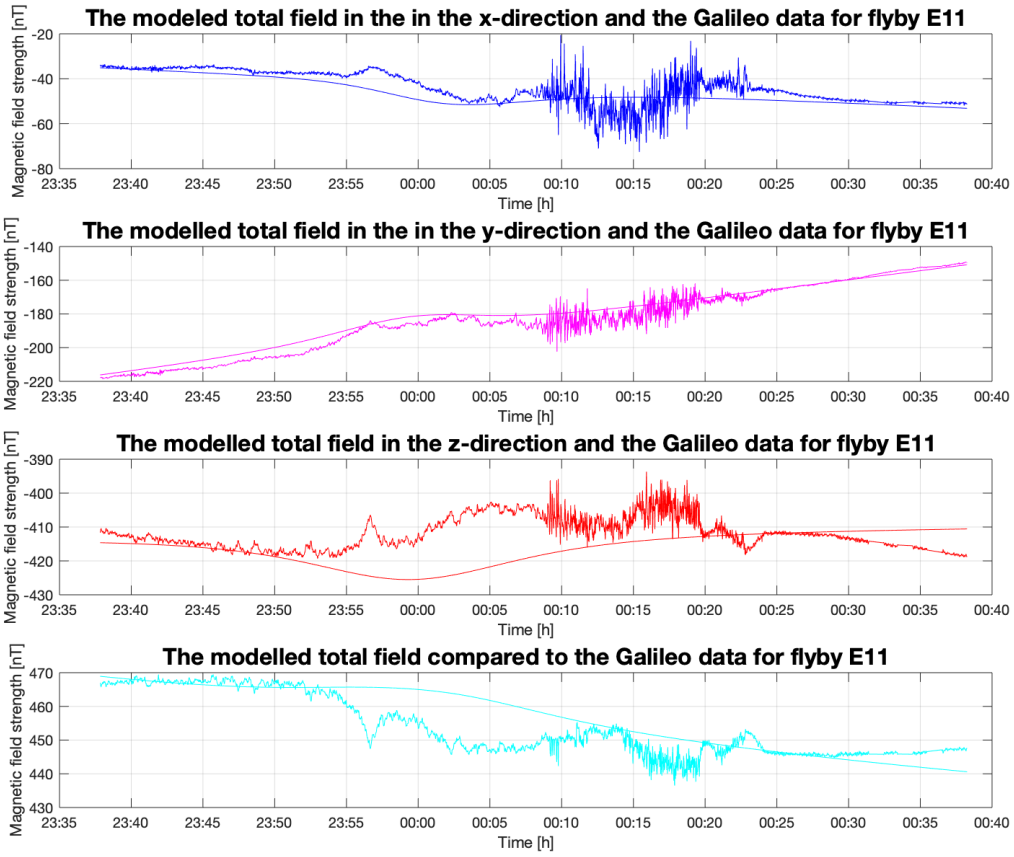

Figure 18: The total magnetic field is calculated using the model. The total field (background and induced field) is presented in each direction (EPHIO coordinates) for the E11 flyby. as well as the total field) for the E11 flyby. The sum of the components (B) is also shown. The model is also compared to the corresponding Galileo-data

5 Summary, conclusion and outlook

To conclude, it can be argued that the model presented in this study provides an **useful and reasonable** picture of the induced field by Europa when it is exposed to Jupiter's time-varying magnetic field. The best fit of the model to the data was shown for Galileo-flyby E4 and E14, and even considering flyby E26 showed poor resolution (few data points), the induction follows the model to some extent.

However, it is **unclear** why earlier papers by Khurana et al. [1998a] and Zimmer et al. [2000] present an almost non-existent z-component of the magnetic field. As can be seen in, for instance, figure 13 and 14, the model presented in this thesis gives a z-component of the magnetic field which matches fairly well with the measured induction. In addition, in figure 13, the difference in amplitude between the model and the data in the z-direction can be explained by impurities in the conductive sheet and its impact on A, the amplitude, since the sheet probably is not homogeneous and cannot be considered an ideal conductor across the whole moon. As seen in figure 17, the amplitude has a great impact on the modeled field and A needs to be constrained further if the exact nature of the sheet is to be determined.

From figure 15, it can be concluded that the assumption of considering the conductive layer as an ocean with a conductivity close to the one of Earths oceans, is valid. In addition, the amplitude of the induced field increases with shell thickness, as seen in figure 16, as expected.

The model can be improved further by adding corrections for plasma currents and Alvén wings, as

well as by constraining the amplitude and phase lag further in the ionosphere of the moon. With this in mind, further research is needed to be able to determine the thickness, h, of the conductive sheet and the exact conductivity, σ. Additionally, if **Ganymede's** and **Callisto** are to be considered we must consider the moon's conductive ionosphere and its effect on the total magnetic field, to be able to study if there exists an ocean below the surface. A conductive ionosphere is not believed to create the whole inductive response but could explain parts of it. Also, **Io** and **Ganymede's** are believed to possess internal dynamos that could have a noticeable effect on the total magnetic field.

Lastly, as shown in this thesis, **the induction model** is arguably a good start with the potential to be adapted to the other Galilean moons, and with the corrections and improvements mentioned above, a good starting point for the coming JUICE mission. JUICE will use passive low-frequency electromagnetic methods to study both the magnetic and electric fields, and investigate the impedance of the moons and the skin depth.

References

J. D. Anderson, E. L. Lau, W. L. Sjogren, G. Schubert, and W. B. Moore. Europa's differentiated internal structure: Inferences from two Galileo encounters. *Science*, 276:1236–1239, May 1997. doi: 10.1126/science.276.5316.1236.

M. Belton. Carr and C. Chapman. Evidence for a subsurface ocean on Europa. *Science*, 391:363–365, 1998. doi: https://doi.org/10.1038/34857.

O. Grasset, Jean-Pierre Lebreton, Michel Blanc, M. Dougherty, C. Erd, R. Greeley, and B. Pappalardo. The jupiter ganymede orbiter as part of the esa/nasa europa jupiter system mission (ejsm). 01 2009.

Robert Grimm, Julie Castillo-Rogez, Carol Raymond, and Andrew R. Poppe. Feasibility of characterizing subsurface brines on Ceres by electromagnetic sounding. Icarus, 362:114424, July 2021. doi: 10.1016/j.icarus.2021.114424.

H Hussmann, P Palumbo, R Jaumann, M Dougherty, Y Langevin, G. Piccioni, S Barabash, P Wurz, P van den Brandt, L Gurvits, L Bruzzone, J Plaut, JE Wahlund, B Cecconi, P Hartogh, R Gladstone, L Iess, DJ Stevenson, Y Kaspi, O Grasset, and L Fletcher. *JUICE JUpiter ICy moons Explorer: Exploring the emergence of habitable worlds around gas giants*, volume ESA/SRE. ESA, 2014. Definition Study Report.

Xianzhe Jia, Margaret G. Kivelson, Krishan K. Khurana, and William S. Kurth. Evidence of a plume on Europa from Galileo magnetic and plasma wave signatures. *Nature Astronomy*, 2:459–464, May 2018. doi: 10.1038/s41550-018-0450-z.

K. K. Khurana, M. G. Kivelson, D. J. Stevenson, G. Schubert, C. T. Russell, R. J. Walker, and C. Polanskey. Induced magnetic fields as evidence for subsurface oceans in Europa and Callisto. Nature, 395(6704):777–780, October 1998a. doi: 10.1038/27394.

K. K. Khurana, M. G. Kivelson, D. J. Stevenson, G. Schubert, C. T. Russell, R. J. Walker, and C. Polanskey. Induced magnetic fields as evidence for subsurface oceans in Europa and Callisto. Nature, 395(6704):777–780, October 1998b. doi: 10.1038/27394.

K. K. Khurana, M. G. Kivelson, K. P. Hand, and C. T. Russell. Electromagnetic Induction from Europa's Ocean and the Deep Interior. In Robert T. Pappalardo, William B. McKinnon, and Krishan K. Khurana, editors, *Europa*, page 571. 2009.

M. G. Kivelson, K. K. Khurana, D. J. Stevenson, L. Bennett, S. Joy, C. T. Russell, R. J. Walker, C. Zimmer, and C. Polanskey. Europa and Callisto: Induced or intrinsic fields in a periodically varying plasma environment. J. Geophys. Res., 104(A3):4609–4626, March 1999. doi: 10.1029/1998JA900095.

Margaret G. Kivelson, Krishan K. Khurana, Christopher T. Russell, Martin Volwerk, Raymond J. Walker, and Christophe Zimmer. Galileo Magnetometer Measurements: A Stronger Case for a Subsurface Ocean at Europa. *Science*, 289(5483):1340–1343, August 2000. doi: 10.1126/science.289.5483.1340.

K. Kuramoto, Y. Saiganji, and T. Yamamoto. Oscillating Magnetic Dipole Moment of Europa Induced by Jovian Magnetic Field: A Possible Probe for Detecting Europa's Ocean. page 1254, March 1998.

NASA/JPL-Caltech. A window into europa's ocean right at the surface. `https://www.nasa.gov/topics/solarsystem/features/europa20130305.html`, 2013. Accessed: may, 2022.

F. M. Neubauer. Alfvén wings and electromagnetic induction in the interiors: Europa and Callisto. J. Geophys. Res., 104(A12):28671–28684, January 1999. doi: 10.1029/1999JA900217.

Carl Nordling and Jonny Österman. *Physics handbook: for science and engineering.* Studentlitteratur, Lund, ninth edition, 2020. ISBN 9144128061;9789144128061;.

W.D. Parkinson. *Introduction to Geomagnetism.* Scottish Academic, Edinburgh, 1983.

Edward M. Purcell and David J. Morin. *Electricity and Magnetism.* Cambridge University Press, third edition, 2013.

E. M. Shoemaker and R. F. Wolfe. Cratering time scales for the Galilean satellites. In *Satellites of Jupiter*, pages 277–339. University of Arizona Press, January 1982.

Christophe Zimmer, Krishan K. Khurana, and Margaret G. Kivelson. Subsurface Oceans on Europa and Callisto: Constraints from Galileo Magnetometer Observations. Icarus, 147(2):329–347, October 2000. doi: 10.1006/icar.2000.6456.

6 Appendix

6.1 Modelled field and data comparison for flyby E11, E12, E14, E15 and E19

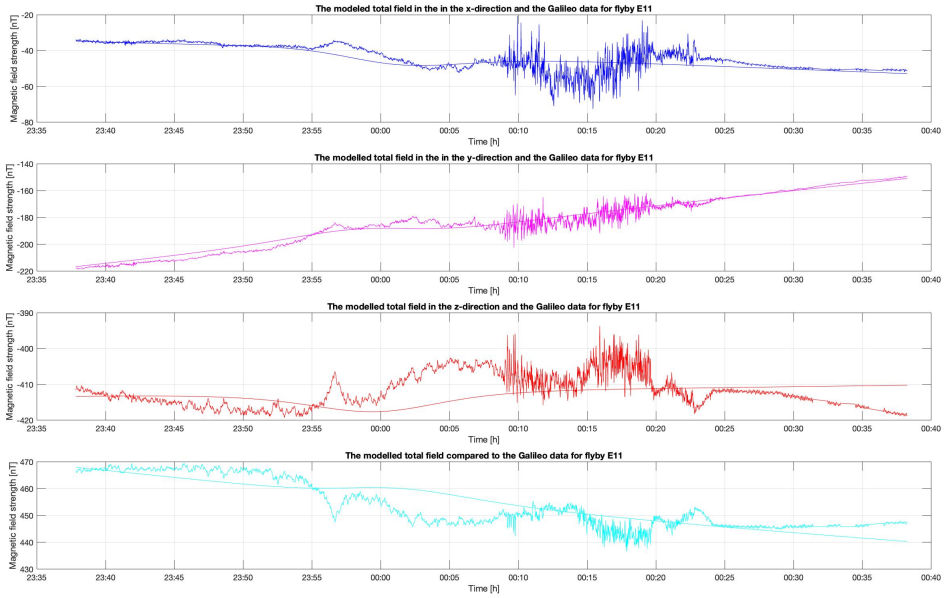

Figure 19: The modelled field for flyby E11, plotted together with the data collected by the Galileo space craft.

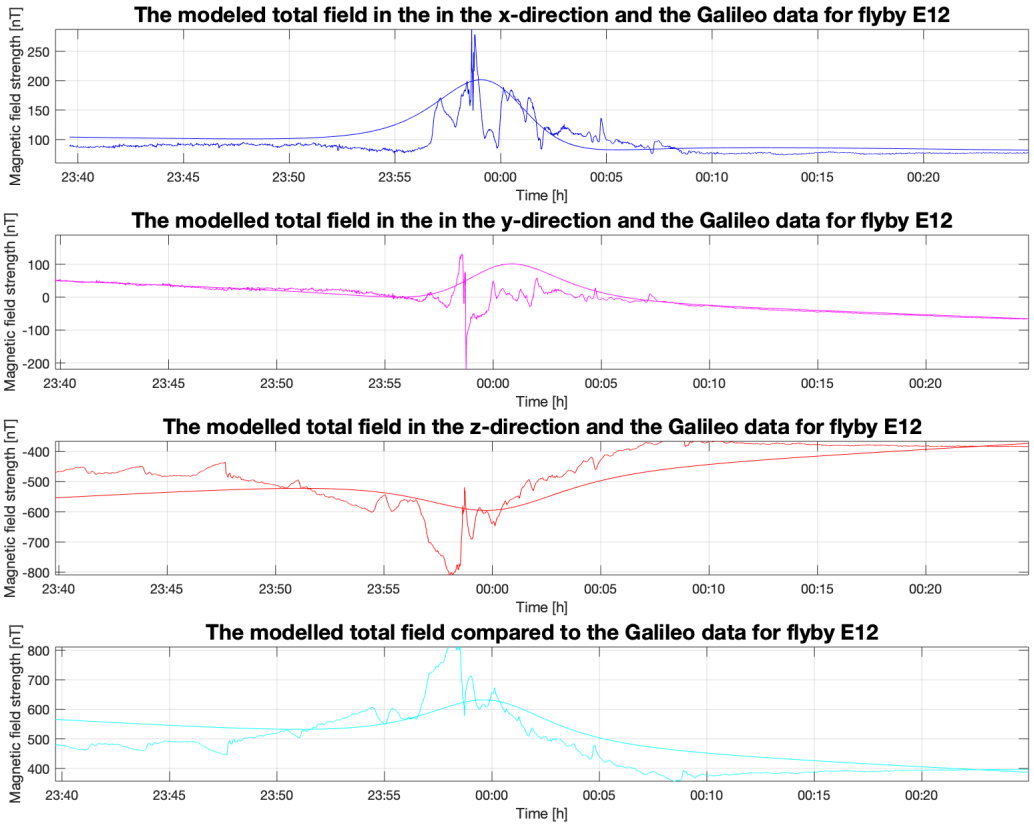

Figure 20: The modelled field for flyby E12, plotted together with the data collected by the Galileo space craft.

6.2 Matlab code

The model was made using Matlab, and the following scripts and functions where used.

6.2.1 Main script

The script below was used to calculate the magnetic field for a whole syndoic period, as well as to extract the closest approach.

```
clear all; close all;

%this is the main script for calculating the magnetic field at Europa, and
%the induced field
%first in Jupiter-centered coordinates (system III) and then in an Europa-centered coordinates (EPHIO)

% definied constants
P=9.8*60*60; %period  [s]
t=(0:P)'; %time  [s]
omega=(2*pi/P);% angular frequency [rad/s]
L=9.5; %jovian radii
lamda=omega*t; %lonitude [rad]
mu_0=1.2566e-6; %permeability of free space [mkgs^-2A^-2]
sigma=2.75; %conductivity for Earths ocean [s/m]
d=50e3; % thickness of the surface ice [m]
```

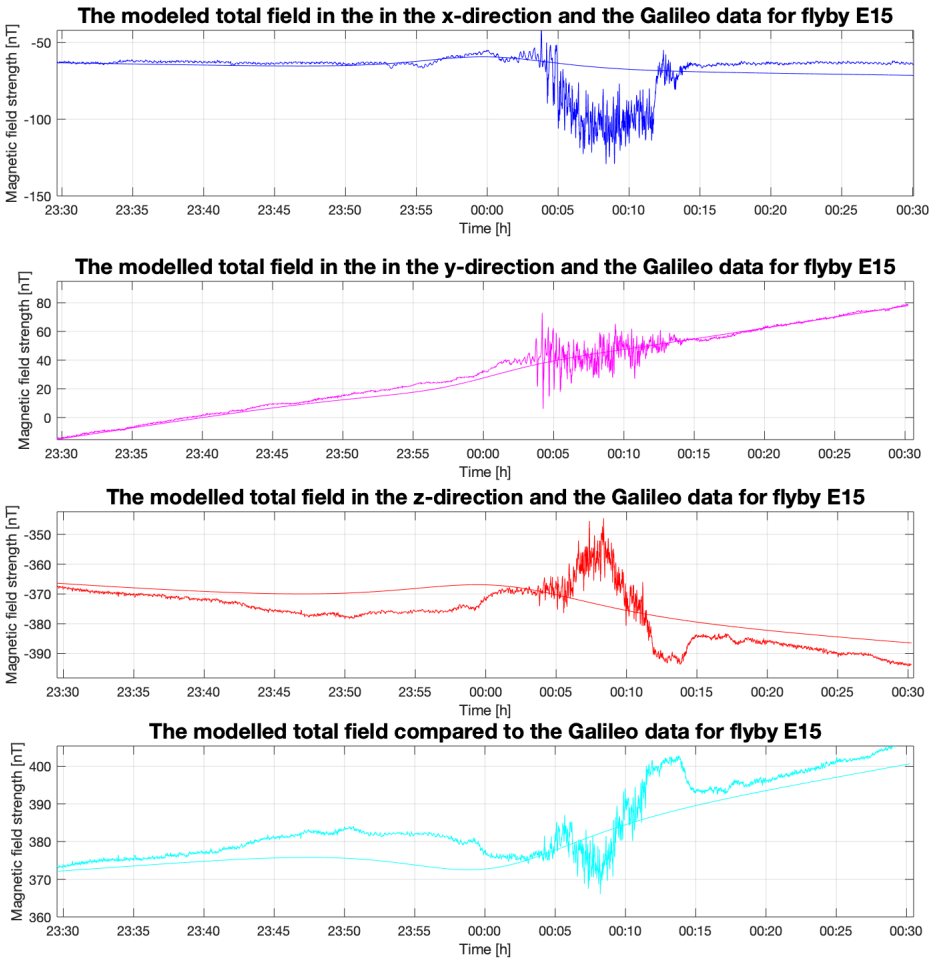

Figure 21: The modelled field for flyby E15, plotted together with the data collected by the Galileo space craft.

```
16 h=100e3; %thickness of ocean layer (conductive layer) [m]
17
18 %position definitions
19 reuropa=1560e3; % radius of moon in [m]
20 r=[0 0 1]'*reuropa; %position vector from Europa-center, ie position
       where we want to calculate the magnetic field
21 r_0=reuropa-d;
22 location='at equator';
23
24
25 %calculates the magnetic field of Jupiter at the position of Europa
26 %(Jupiter system III coordinates)
27 B=Jupiter_Magfield(L, lamda); %[nT]
28
29 Bprime=[-B(:,1), -B(:,2), B(:,3)]; %magnetic field of Jupiter in Europa
       coordinates [B_theta, -B_r, B_phi] <=> [Bx, -By, Bz]
30 B_prime=Bprime;%.*exp(-omega*t);
31 %Calculates the induced magnetic field in Europa coordinates
32
33 B_sec=europainduction(r, sigma, h, d, B_prime, omega);
34
35
36 %% plots the primary and secondary magnetic field in Europa coordinates
```

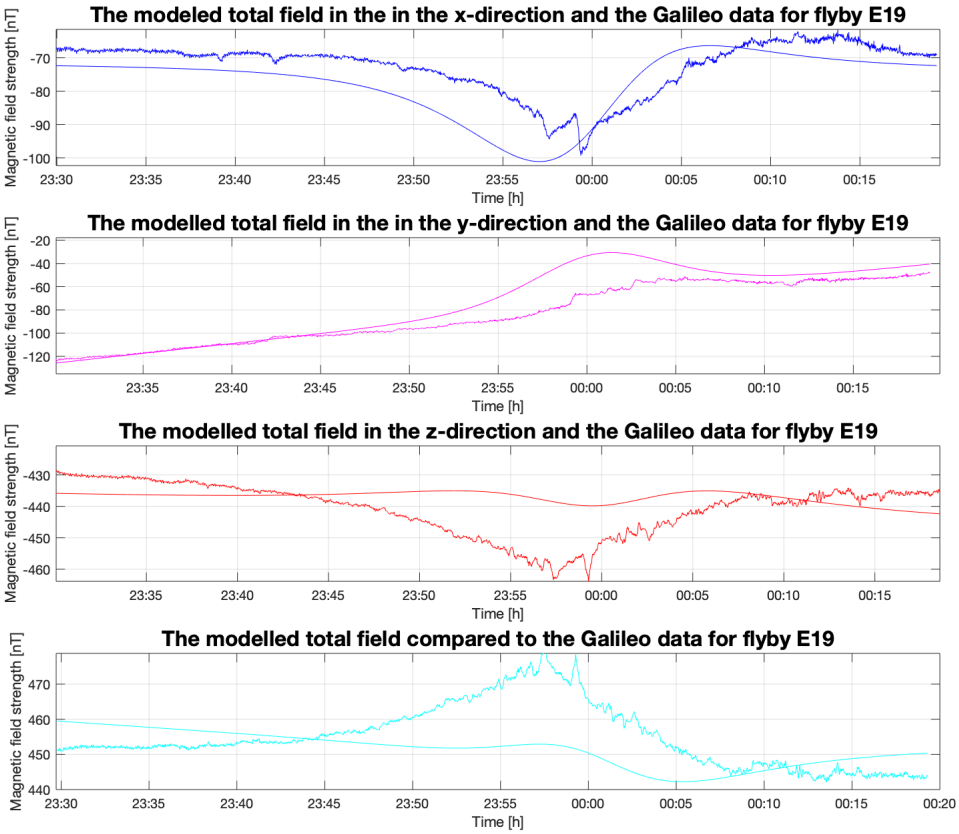

Figure 22: The modelled field for flyby E19, plotted together with the data collected by the Galileo space craft.

```
figure(1);

plot(t/3600, B_prime(:,1),'b')
hold on

plot(t/3600, B_prime(:,2),'k')
plot(t/3600, B_prime(:,3), 'r')

plot(t/3600, B_sec(:,1), 'b--')
plot(t/3600, B_sec(:,2), 'k--')
plot(t/3600, B_sec(:,3), 'r--')

xlabel('Time [h]')
ylabel('Magnetic field strength [nT]')
title("Primary and secondary field in Europa coordinates "+location+"")
legend('B_{primx}', 'B_{primy}', 'B_{primz}', 'B_{secx}', 'B_{secy}', '
    B_{secz}')
grid on

hold off


%% plot of theoretical field with trajectory from space craft

```

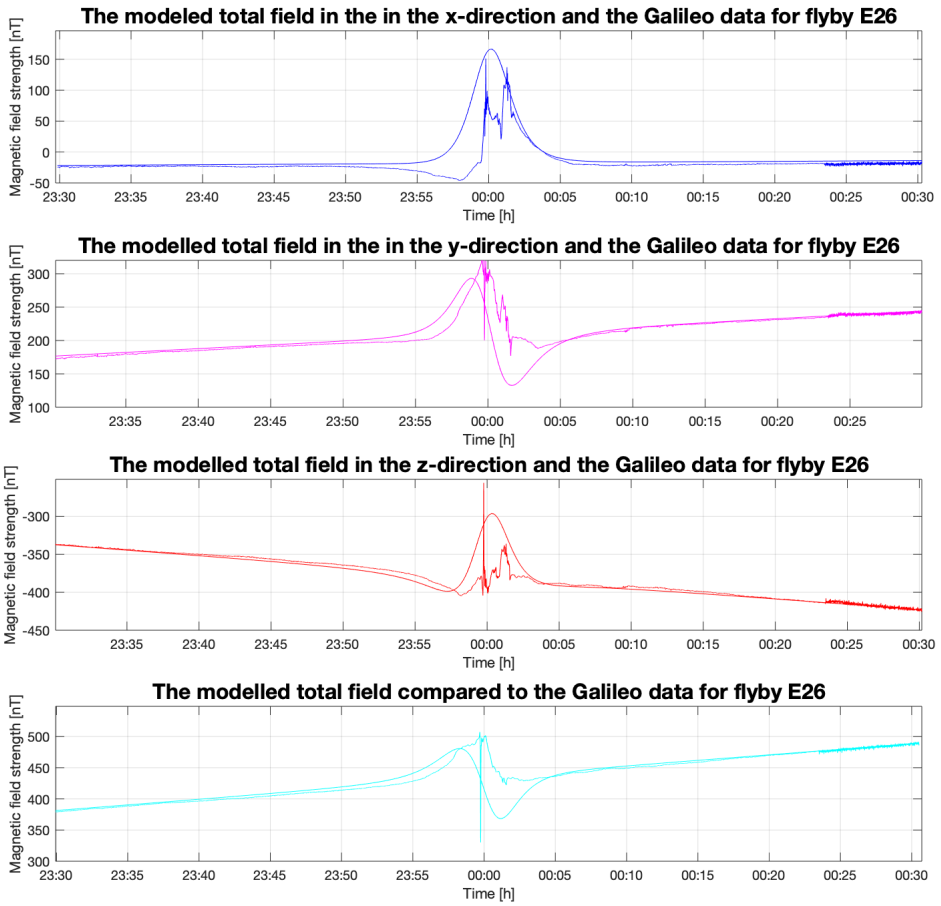

Figure 23: The modelled field for flyby E26, plotted together with the data collected by the Galileo space craft.

```
%read data
data_ephio = read_galileo_MAG(4,'EPHIO');
%    EPHIO: time Bx By Bz |B|[nT] X_RE Y_RE Z_RE

data_sys3 = read_galileo_MAG(4,'SYS3');
%    SYS3:  time Br Btheta Bphi |B|[nT] R[R_E] Lat[deg] ELong[deg] Wlong
    [deg]

%position coordinates from data
rx=data_ephio(:,6)*reuropa;
ry=data_ephio(:,7)*reuropa;
rz=data_ephio(:,8)*reuropa;

r_traj=[rx ry rz];

%magnetic field from data
bx=data_ephio(:,2);
by=data_ephio(:,3);
bz=data_ephio(:,4);

b=[bx by bz];

b_abs=sqrt(b(:,1).^2+b(:,2).^2+b(:,3).^2);

```

```
%length of position vector for space craft
r_sc=sqrt(rx.^2+ry.^2 +rz.^2);% in Europa radii
t_sc=data_ephio(:,1); %time for space craft

%plot to find the closest approach point

figure(2);

plot(t_sc, r_sc)
flyby='E4'; %change for different flybys
date='1996 -12-19';

xlabel('Time')
ylabel('Position [m]')
title("Trajectory of space craft for the "+flyby+" ("+date+")")
legend('r')
grid on
datetick

%time in Jupiter sys III and extraction of longitude
t_ju=data_sys3(:,1);
longeast=data_sys3(:,8);
longwest=data_sys3(:,9);

%ca=closest approach
r_ca=min(r_sc);
t_ca=find(r_sc==r_ca);

%plot to find the east longitude at closest approach
figure(3);
plot(t_ju,longeast)
hold on

plot(t_ju, longwest)
hold off
grid on
xlabel('Time')
ylabel('Longitude [degrees]')
title('Extrapolation of longitude from time')
legend('east longitude', 'west longitude')
datetick

%calculation of the induced magnetic field for trajectory of space craft

longitude=(longeast(t_ca)*pi)/180; %longitude in radians

Bp=Jupitertrajectory(L, longitude); %calls for function to calcualte the
    primary field from Ju iter
Bp=[-Bp(1), -Bp(2), Bp(3)]; %changes coordinates to EPHIO
Bs=inductiontrajectory(r, sigma,  h, d, Bp, omega); %calls for function
   to calculate the secondary field at time of closest encounter



%theoretical magnetic field for given trajectory
%time=[t_ca-1200:t_ca+1200]; %time in [s]
time=data_ephio(:,1);
t0=time(t_ca); %time for closest approach
```

```
time=time-time(t_ca);
time=time*24*3600; %[s]


lamda=longitude + omega*time(:,1);

B = Magfield(L, lamda);
B_p=[-B(:,1) -B(:,2) B(:,3)];



B_s=induction(r_traj, sigma,  h, d, B_p, omega);

B_sum=B_p+B_s;
B_abs=sqrt(B_sum(:,1).^2+B_sum(:,2).^2+B_sum(:,3).^2);

time=time/(3600*24);
time=time+t0;

%plot to compare data with model

figure(4);

hold on


plot(time, b(:,1),'b')
hold on

plot(time, b(:,2),'k')
plot(time, b(:,3), 'r')
plot(time, b_abs, 'c')

plot(time, B_sum(:,1), 'b')
plot(time, B_sum(:,2), 'k')
plot(time, B_sum(:,3), 'r')
plot(time, B_abs, 'c')


xlabel('Time [h]')
ylabel('Magnetic field strength [nT]')
title('Comparision between model and Galileo data')
legend('B_{x}', 'B_{y}', 'B_{z}', 'B_{x}', 'B_{y}', 'B_{z}')

grid on
datetick
hold off
```

6.2.2 Comparison of model and data

The script below was the mains script to compare the model to the data.

```
%script to estimate the backgroudn field and calculate the induced field
%at the space craft. The theoretical field is compared to data collected
    by
%the Galileo space probe

clear all; close all;

```

```
7
8  % definied constants
9  P=11.1*60*60; %synodic period 11.1 h for Europa  (Khurana et al. 1998) [
       s]
10 omega=(2*pi/P);% angular frequency [rad/s]
11 L=9.5; %jovian radii
12 mu_0=1.2566e-6; %permeability of free space [mkgs^-2A^-2]
13 sigma=2.75; %conductivity for Earths ocean at 0 degrees [s/m]
14 d=50e3; % thickness of the surface ice [m]
15 h=100e3; %thickness of ocean layer (conductive layer) [m]
16
17
18 %position definitions
19 reuropa=1560e3; % radius of Europa in [m]
20 flyby='E19'; % label of flyby [E4  E11 E12 E14 E15 E17 E19 E26]
21
22 %read data
23 data_ephio = read_galileo_MAG(19,'EPHIO');
24 %    EPHIO: time Bx By Bz |B|[nT] X_RE Y_RE Z_RE
25
26 data_sys3 = read_galileo_MAG(19,'SYS3');
27 %    SYS3:  time Br Btheta Bphi |B|[nT] R[R_E] Lat[deg] ELong[deg] Wlong
       [deg]
28
29 %position coordinates of space craft from data
30 rx=data_ephio(:,6)*reuropa;
31 ry=data_ephio(:,7)*reuropa;
32 rz=data_ephio(:,8)*reuropa;
33 r_traj=[rx ry rz];
34
35 %length of space craft vector
36 for n=1:size(r_traj)
37 r_sc(n)=sqrt(r_traj(n,1).^2+r_traj(n,2).^2+r_traj(n,3).^2);% in Europa
       radii
38 end
39
40 r_sc=r_sc';
41
42 %magnetic field from data in EPHIO coordinates from data
43 bx=data_ephio(:,2);
44 by=data_ephio(:,3);
45 bz=data_ephio(:,4);
46 b=[bx by bz];
47
48 b_abs=sqrt(b(:,1).^2+b(:,2).^2+b(:,3).^2); %length of magnetic field
       vector
49
50 %time-vector from data
51 t_sc=data_ephio(:,1);
52
53 %time in Jupiter sys III and extraction of longitude
54 t_ju=data_sys3(:,1);
55 longeast=data_sys3(:,8);
56 longwest=data_sys3(:,9);
57
58 %extraction of the c/a (i.e. closest approach)
59 r_ca=min(r_sc);
60 t_ca=find(r_sc==r_ca);
```

```
61 t0=t_ca; %normalization point
62
63 %calculation of the induced magnetic field for trajectory of space craft
64 longitude=((longeast(t_ca))*pi)/180; %longitude at c/a in radians
65
66 %extraction of time and normalization with respect to tc/a
67 time=data_ephio(:,1); %time=[t_ca-1200:t_ca+1200]; %time in [s]
68 time=time-time(t_ca); %remove point of c/a
69 time=time*24*3600; % scale of time [s]
70
71 %shift of location where Europa is located with respect to Jupiter
72 lamda=longitude + omega*time(:,1); %shift of the longitude
73 B_europa_sys3 = Magfield(9.5, lamda); %the primary field at Europa
74 B_europa_ephio=[B_europa_sys3(:,1) -B_europa_sys3(:,2) B_europa_sys3
       (:,3)]; %change from Jup Sys III to EPHIO
75 B_europa_prime=B_europa_ephio;
76 %B_europa_prime(:,3)=zeros(size(B_europa_ephio(:,1)));
77
78 %calculation of magnetic moment (M) and, from this, the induced field (
       B_s)
79 M=induction(r_traj, sigma,  h, d, B_europa_prime, omega);
80
81 constant=mu_0/(4*pi);
82
83 for n=1:size(r_traj)
84     rnorm(n)=sqrt(r_traj(n,1).^2+r_traj(n,2).^2+r_traj(n,3).^2);
85 end
86
87 rnorm=rnorm';
88 r2=rnorm.^2;
89 r5=rnorm.^5;
90 rdotM=dot(r_traj,M,2);
91
92 %secondary field at space craft
93 for n=1:size(r_traj)
94
95     B_s(n,:)=(constant.*((3.*rdotM(n).*r_traj(n,:))-(r2(n).*M(n,:)))./
           r5(n);
96
97 end
98
99 B_s=[B_s(:,1) B_s(:,2) -B_s(:,3)]; %collection of magnetic field
100
101
102 %Estimation of the background field usinng a linear fit of data
103 P1 = polyfit(data_ephio(:,1),data_ephio(:,2),1);
104 P2 = polyfit(data_ephio(:,1),data_ephio(:,3),1);
105 P3 = polyfit(data_ephio(:,1),data_ephio(:,4),1);
106
107 B1 = data_ephio(:,1).*P1(1) + P1(2);
108 B2 = data_ephio(:,1).*P2(1) + P2(2);
109 B3 = data_ephio(:,1).*P3(1) + P3(2);
110
111 %the background field at the space craft
112 B_p = [B1 B2 B3];
113
114 %total theoretical field
115 B_sum=B_p+B_s;
```

```
116
117 %length of total field
118 B_abs=sqrt(B_sum(:,1).^2+B_sum(:,2).^2+B_sum(:,3).^2);
119
120 %re-scale of time
121 time=time/(3600*24);
122 time=time+t0;
123
124 %plot of model and data
125
126 subplot(4,1,1)
127 plot(time, B_sum(:,1), 'b')
128 hold on
129 plot(time, b(:,1), 'b')
130 %plot(time, B_europa_ephio(:,1),'b')
131
132 xlabel('Time [h]')
133 ylabel('Magnetic field strength [nT]')
134 title("The modeled total field in the in the x-direction and the Galileo
      data for flyby "+flyby+"")
135 grid on
136 datetick
137
138 subplot(4,1,2);
139 plot(time, B_sum(:,2), 'm')
140 hold on
141 plot(time, b(:,2), 'm')
142 %plot(time, B_europa_ephio(:,2),'m')
143
144 xlabel('Time [h]')
145 ylabel('Magnetic field strength [nT]')
146 title("The modelled total field in the in the y-direction and the
     Galileo data for flyby "+flyby+""')
147 grid on
148 datetick
149
150 subplot(4,1,3)
151
152 plot(time, B_sum(:,3), 'r')
153 hold on
154 plot(time, b(:,3), 'r')
155 %plot(time, B_europa_ephio(:,3),'r')
156
157 xlabel('Time [h]')
158 ylabel('Magnetic field strength [nT]')
159 title("The modelled total field in the z-direction and the Galileo data
     for flyby "+flyby+"")
160 grid on
161 datetick
162
163 subplot(4,1,4)
164
165 plot(time, B_abs, 'c')
166 hold on
167 plot(time, b_abs, 'c')
168
169 xlabel('Time [h]')
170 ylabel('Magnetic field strength [nT]')
```

```
171 title('The modelled total field compared to the Galileo data for flyby
      "+flyby+"')
172
173 grid on
174 datetick
```

6.2.3 Function to calculate theoretical background field

```
1  function B = Magfield(L, lamda)
2
3  % calculate the magnetic field at equator-plane of Jupiter system III
4  % Jovian spherical coordinates
5  % Jupiter_Magfield(L, lamda)
6  % L: distance from Jupiter in RJ (Jovii radii)
7  % Lamda= omega*t in system III, degrees
8
9       in= 9.6; % magnetic dipole inclination angle in degrees
10      B_DJ= 417e-6; %the magnetic field at the equator [T]
11
12      B_Dtheta =     B_DJ*cosd(in)*L.^(-3).*ones(size(lamda)); %B_z
13      B_Dr     = 2 *B_DJ*sind(in)*L.^(-3).*cos(lamda); % -B_y
14      B_Dphi   =   -B_DJ*sind(in)*L.^(-3).*sin(lamda); % B_x
15      %B_tot=sqrt(B_Dtheta.^2+B_Dr.^2+B_Dphi.^2);
16
17      B=[B_Dphi, B_Dr, B_Dtheta]*1e9; %[nT] in Jupiter coodinates
18
19
20
21 end
```

6.2.4 Function to calculate the induced field

```
1  %convert Bprime in Europa coordinates at one position
2  function M=induction(r_traj, sigma,  h, d, B_europa, omega)
3
4
5  r_m=1560e3 ; %radius in m
6  r_0=r_m-d;
7  r_1=r_m-d-h;
8  mu_0=1.2566e-6; %permeability of free space [mkgs^-2A^-2]
9
10
11 k=(1-1i)*sqrt(mu_0*sigma*omega/2);
12
13
14
15 f1=r_0*k;
16 f2=r_1*k;
17
18 %form besselj(NU, Z) where z can be complex
19 J1=besselj(5/2,f1) ;
20 J2=besselj(-5/2,f1) ;
21 J3=besselj(1/2,f1) ;
22 J4=besselj(-1/2,f1) ;
23 J5=besselj(-5/2, f2);
24 J6=besselj(3/2, f2);
25 J7=besselj(1/2,f2);
26
27 R=(r_1.*k*J5)/((3*J6)-(r_1.*k*J7));
```

```
28
29
30 A=(r_0/r_m)^3.*(((R*J1)-J2)/((R*J3)-J4)); %amplitude
31
32
33 for n=1:size(B_europa)
34
35     M(n,:)=-((4*pi)/mu_0).*A.*B_europa(n,:)*(r_m^3/2); %induced magnetic
           dipole moment
36
37 end
38
39
40 end
```

6.2.5 Script to change the ammplitude factor, A

```
1  %change  A
2
3
4  hold all
5  % definied constants
6  P=11.1*60*60; %synodic period 11.1 h for Europa, 10.1 h for Callissto (
       Khurana et al. 1998) [s]
7  omega=(2*pi/P);% angular frequency [rad/s]
8  L=9.5; %jovian radii
9  mu_0=1.2566e-6; %permeability of free space [mkgs^-2A^-2]
10 sigma=2.75; %conductivity for Earths ocean at 0 degrees [s/m]
11 d=50e3; % thickness of the surface ice [m]
12 h=100e3; %thickness of ocean layer (conductive layer) [m]
13
14
15
16 %position definitions
17 reuropa=1560e3; % radius of moon in [m]
18 flyby='E4';
19 %in data E4  E11 E12 E14 E15 E17 E19 E26
20 %read data
21 data_ephio = read_galileo_MAG(4,'EPHIO');
22 %    EPHIO: time Bx By Bz |B|[nT] X_RE Y_RE Z_RE
23
24 data_sys3 = read_galileo_MAG(4,'SYS3');
25 %    SYS3:  time Br Btheta Bphi |B|[nT] R[R_E] Lat[deg] ELong[deg] Wlong
       [deg]
26
27 %position coordinates from data
28 rx=data_ephio(:,6)*reuropa;
29 ry=data_ephio(:,7)*reuropa;
30 rz=data_ephio(:,8)*reuropa;
31 r_traj=[rx ry rz];
32 %magnetic field from data in EPHIO
33 bx=data_ephio(:,2);
34 by=data_ephio(:,3);
35 bz=data_ephio(:,4);
36 b=[bx by bz];
37
38 %time from data
39 t_sc=data_ephio(:,1);
40
```

```
41 A=-[0.1  0.4  0.6  0.8  1.0  1.2  1.4  1.6];
42
43 for q=1:8
44
45
46 %length of vectors
47 b_abs=sqrt(b(:,1).^2+b(:,2).^2+b(:,3).^2);
48
49 for n=1:size(r_traj)
50 r_sc(n)=sqrt(r_traj(n,1).^2+r_traj(n,2).^2+r_traj(n,3).^2);% in Europa
       radii
51 end
52
53 r_sc=r_sc';
54
55 %time in Jupiter sys III and extraction of longitude
56 t_ju=data_sys3(:,1);
57 longeast=data_sys3(:,8);
58 longwest=data_sys3(:,9);
59
60 %ca=closest approach
61 r_ca=min(r_sc);
62 t_ca=find(r_sc==r_ca);
63 t0=t_ca;
64
65 %calculation of the induced magnetic field for trajectory of space craft
66 longitude=((longeast(t_ca))*pi)/180; %longitude at c/a in radians
67
68 %extraction of time and normalization with respect to tc/a
69 time=data_ephio(:,1); %time=[t_ca-1200:t_ca+1200]; %time in [s]
70 time=time-time(t_ca); %remove point of c/a
71 time=time*24*3600; % scale of time [s]
72
73 %shift of location where Europa is located with respect to Jupiter
74 lamda=longitude + omega*time(:,1); %shift of the longitude
75 B_europa_sys3 = Magfield(9.5, lamda); %the primary field at Europa
76 B_europa_ephio=[B_europa_sys3(:,1) -B_europa_sys3(:,2) B_europa_sys3
       (:,3)]; %change from Jup Sys III to EPHIO
77 B_europa_prime=B_europa_ephio;
78 B_europa_prime(:,3)=zeros(size(B_europa_ephio(:,1)));
79
80 %calculation of seconday field
81 M=inductionA(r_traj, sigma,  h, d, B_europa_prime, omega, A(q));
82
83
84 constant=mu_0/(4*pi);
85
86 for n=1:size(r_traj)
87     rnorm(n)=sqrt(r_traj(n,1).^2+r_traj(n,2).^2+r_traj(n,3).^2);
88 end
89
90 rnorm=rnorm';
91 r2=rnorm.^2;
92 r5=rnorm.^5;
93 rdotM=dot(r_traj,M,2);
94
95 %secondary field at space craft
96 for n=1:size(r_traj)
```

```
97
98      B_s(n,:)=(constant.*((3.*rdotM(n).*r_traj(n,:))-(r2(n).*M(n,:)))./
            r5(n);
99
100 end
101
102 B_s=[B_s(:,1) B_s(:,2) -B_s(:,3)];
103
104
105 %Calculation of empirical B-field from linear fit of data
106 P1 = polyfit(data_ephio(:,1),data_ephio(:,2),1);
107 P2 = polyfit(data_ephio(:,1),data_ephio(:,3),1);
108 P3 = polyfit(data_ephio(:,1),data_ephio(:,4),1);
109
110 B1 = data_ephio(:,1).*P1(1) + P1(2);
111 B2 = data_ephio(:,1).*P2(1) + P2(2);
112 B3 = data_ephio(:,1).*P3(1) + P3(2);
113
114 %the primary field at the space craft
115
116 B_p = [B1 B2 B3];
117
118
119 %total theoretical field
120 B_sum=B_p+B_s;
121
122 %length of total field
123 B_abs=sqrt(B_sum(:,1).^2+B_sum(:,2).^2+B_sum(:,3).^2);
124
125 %re-scale of time
126 time=time/(3600*24);
127 time=time+t0;
128
129 %plot of model for different amplitude
130
131
132
133 subplot(3,1,1)
134 l=plot(time, B_sum(:,1));
135 legends{q} = sprintf(['Amplitude ' num2str(A(q)) '']) ;
136 hold on
137 plot(time, b(:,1))
138 datetick
139 grid on
140
141 xlabel('Time [h]')
142 ylabel('Magnetic field strength [nT]')
143 title("The modelled field for different amplitude factors (A) for the "+
        flyby+" flyby in the x-direction")
144
145 subplot(3,1,2);
146 plot(time, B_sum(:,2))
147 hold on
148 plot(time, b(:,2))
149 datetick
150 grid on
151
152 xlabel('Time [h]')
```

```
153 ylabel('Magnetic field strength [nT]')
154 title("The modelled field for different amplitude factors (A) for the "+
    flyby+" flyby in the y-direction")
155
156 subplot(3,1,3);
157 plot(time, B_sum(:,3))
158 hold on
159 plot(time, b(:,3))
160 datetick
161 grid on
162
163 xlabel('Time [h]')
164 ylabel('Magnetic field strength [nT]')
165 title("The modelled field for different amplitude factors (A) for the "+
    flyby+" flyby in the z-direction")
166
167 end
168
169 legend(legends)
```

6.2.6 Script to change the conductivity of the conductive layer

```
1  %script to compare data with model
2  %clear all; close all;
3  hold all
4  % definied constants
5  P=11.1*60*60; %synodic period 11.1 h for Europa, 10.1 h for Callissto (
       Khurana et al. 1998) [s]
6  omega=(2*pi/P);% angular frequency [rad/s]
7  L=9.5; %jovian radii
8  mu_0=1.2566e-6; %permeability of free space [mkgs^-2A^-2]
9  %sigma=2.75; %conductivity for Earths ocean at 0 degrees [s/m]
10 d=50e3; % thickness of the surface ice [m]
11 h=100e3; %thickness of ocean layer (conductive layer) [m]
12
13
14
15 %position definitions
16 reuropa=1560e3; % radius of moon in [m]
17 flyby='E4';
18 %in data E4  E11 E12 E14 E15 E17 E19 E26
19 %read data
20 data_ephio = read_galileo_MAG(4,'EPHIO');
21 %    EPHIO: time Bx By Bz |B|[nT] X_RE Y_RE Z_RE
22
23 data_sys3 = read_galileo_MAG(4,'SYS3');
24 %    SYS3:  time Br Btheta Bphi |B|[nT] R[R_E] Lat[deg] ELong[deg] Wlong
       [deg]
25
26 %position coordinates from data
27 rx=data_ephio(:,6)*reuropa;
28 ry=data_ephio(:,7)*reuropa;
29 rz=data_ephio(:,8)*reuropa;
30 r_traj=[rx ry rz];
31 %magnetic field from data in EPHIO
32 bx=data_ephio(:,2);
33 by=data_ephio(:,3);
34 bz=data_ephio(:,4);
35 b=[bx by bz];
```

```
36
37 %time from data
38 t_sc=data_ephio(:,1);
39
40 sigma=[1 2.75 10 100 200 300 400 500];
41
42 for q=1:8
43
44
45 %length of vectors
46 b_abs=sqrt(b(:,1).^2+b(:,2).^2+b(:,3).^2);
47
48 for n=1:size(r_traj)
49 r_sc(n)=sqrt(r_traj(n,1).^2+r_traj(n,2).^2+r_traj(n,3).^2);% in Europa
       radii
50 end
51
52 r_sc=r_sc';
53
54 %time in Jupiter sys III and extraction of longitude
55 t_ju=data_sys3(:,1);
56 longeast=data_sys3(:,8);
57 longwest=data_sys3(:,9);
58
59 %ca=closest approach
60 r_ca=min(r_sc);
61 t_ca=find(r_sc==r_ca);
62 t0=t_ca;
63
64 %calculation of the induced magnetic field for trajectory of space craft
65 longitude=((longeast(t_ca))*pi)/180; %longitude at c/a in radians
66
67 %extraction of time and normalization with respect to tc/a
68 time=data_ephio(:,1); %time=[t_ca-1200:t_ca+1200]; %time in [s]
69 time=time-time(t_ca); %remove point of c/a
70 time=time*24*3600; % scale of time [s]
71
72 %shift of location where Europa is located with respect to Jupiter
73 lamda=longitude + omega*time(:,1); %shift of the longitude
74 B_europa_sys3 = Magfield(9.5, lamda); %the primary field at Europa
75 B_europa_ephio=[B_europa_sys3(:,1) -B_europa_sys3(:,2) B_europa_sys3
       (:,3)]; %change from Jup Sys III to EPHIO
76 B_europa_prime=B_europa_ephio;
77 B_europa_prime(:,3)=zeros(size(B_europa_ephio(:,1)));
78
79 %calculation of seconday field
80 M=induction(r_traj, sigma(q), h, d, B_europa_prime, omega);
81
82
83 constant=mu_0/(4*pi);
84
85 for n=1:size(r_traj)
86     rnorm(n)=sqrt(r_traj(n,1).^2+r_traj(n,2).^2+r_traj(n,3).^2);
87 end
88
89 rnorm=rnorm';
90 r2=rnorm.^2;
91 r5=rnorm.^5;
```

```
92  rdotM=dot(r_traj,M,2);
93
94  %secondary field at space craft
95  for n=1:size(r_traj)
96
97      B_s(n,:)=(constant.*((3.*rdotM(n).*r_traj(n,:))-(r2(n).*M(n,:)))./
        r5(n);
98
99  end
100
101 B_s=[B_s(:,1) B_s(:,2) B_s(:,3)];
102
103
104 %Calculation of empirical B-field from linear fit of data
105 P1 = polyfit(data_ephio(:,1),data_ephio(:,2),1);
106 P2 = polyfit(data_ephio(:,1),data_ephio(:,3),1);
107 P3 = polyfit(data_ephio(:,1),data_ephio(:,4),1);
108
109 B1 = data_ephio(:,1).*P1(1) + P1(2);
110 B2 = data_ephio(:,1).*P2(1) + P2(2);
111 B3 = data_ephio(:,1).*P3(1) + P3(2);
112
113 %the primary field at the space craft
114
115 B_p = [B1 B2 B3];
116
117
118 %total theoretical field
119 B_sum=B_p+B_s;
120
121 %length of total field
122 B_abs=sqrt(B_sum(:,1).^2+B_sum(:,2).^2+B_sum(:,3).^2);
123
124 %re-scale of time
125 time=time/(3600*24);
126 time=time+t0;
127
128 %plot of model for different conductivities
129
130
131
132 subplot(3,1,1)
133 plot(time, B_sum(:,1));
134 hold on
135 plot(time, b(:,1))
136 datetick
137 grid on
138 legends{q} = sprintf(['Conductivity ' num2str(sigma(q)) ' [S/m]']) ;
139
140 xlabel('Time [h]')
141 ylabel('Magnetic field strength [nT]')
142 title("The modelled field for different conductivities for the "+flyby+"
        flyby in the x-direction")
143
144 subplot(3,1,2);
145 plot(time, B_sum(:,2))
146 hold on
147 plot(time, b(:,2))
```

```
148 datetick
149 grid on
150
151 xlabel('Time [h]')
152 ylabel('Magnetic field strength [nT]')
153 title("The modelled field for different conductivities for the "+flyby+"
        flyby in the y-direction")
154
155 subplot(3,1,3);
156 plot(time, B_sum(:,3))
157 hold on
158 plot(time, b(:,3))
159 datetick
160 grid on
161
162 xlabel('Time [h]')
163 ylabel('Magnetic field strength [nT]')
164 title("The modelled field for different conductivities for the "+flyby+"
        flyby in the z-direction")
165
166 end
167
168 legend(legends)
```

6.2.7 Script to change the shell thickness

```
1  %change  h
2
3
4  hold all
5  % definied constants
6  P=11.1*60*60; %synodic period 11.1 h for Europa, 10.1 h for Callissto (
       Khurana et al. 1998) [s]
7  omega=(2*pi/P);% angular frequency [rad/s]
8  L=9.5; %jovian radii
9  mu_0=1.2566e-6; %permeability of free space [mkgs^-2A^-2]
10 sigma=2.75; %conductivity for Earths ocean at 0 degrees [s/m]
11 d=50e3; % thickness of the surface ice [m]
12 %h=100e3; %thickness of ocean layer (conductive layer) [m]
13
14
15
16 %position definitions
17 reuropa=1560e3; % radius of moon in [m]
18 flyby='E4';
19 %in data E4  E11 E12 E14 E15 E17 E19 E26
20 %read data
21 data_ephio = read_galileo_MAG(4,'EPHIO');
22 %    EPHIO: time Bx By Bz |B|[nT] X_RE Y_RE Z_RE
23
24 data_sys3 = read_galileo_MAG(4,'SYS3');
25 %    SYS3:  time Br Btheta Bphi |B|[nT] R[R_E] Lat[deg] ELong[deg] Wlong
       [deg]
26
27 %position coordinates from data
28 rx=data_ephio(:,6)*reuropa;
29 ry=data_ephio(:,7)*reuropa;
30 rz=data_ephio(:,8)*reuropa;
31 r_traj=[rx ry rz];
```

```
%magnetic field from data in EPHIO
bx=data_ephio(:,2);
by=data_ephio(:,3);
bz=data_ephio(:,4);
b=[bx by bz];

%time from data
t_sc=data_ephio(:,1);

h=[1 2 3 4 5 6 7  8 9]*10^3;

for q=1:8


%length of vectors
b_abs=sqrt(b(:,1).^2+b(:,2).^2+b(:,3).^2);

for n=1:size(r_traj)
r_sc(n)=sqrt(r_traj(n,1).^2+r_traj(n,2).^2+r_traj(n,3).^2);% in Europa
    radii
end

r_sc=r_sc';

%time in Jupiter sys III and extraction of longitude
t_ju=data_sys3(:,1);
longeast=data_sys3(:,8);
longwest=data_sys3(:,9);

%ca=closest approach
r_ca=min(r_sc);
t_ca=find(r_sc==r_ca);
t0=t_ca;

%calculation of the induced magnetic field for trajectory of space craft
longitude=((longeast(t_ca))*pi)/180; %longitude at c/a in radians

%extraction of time and normalization with respect to tc/a
time=data_ephio(:,1); %time=[t_ca-1200:t_ca+1200]; %time in [s]
time=time-time(t_ca); %remove point of c/a
time=time*24*3600; % scale of time [s]

%shift of location where Europa is located with respect to Jupiter
lamda=longitude + omega*time(:,1); %shift of the longitude
B_europa_sys3 = Magfield(9.5, lamda); %the primary field at Europa
B_europa_ephio=[B_europa_sys3(:,1) -B_europa_sys3(:,2) B_europa_sys3
    (:,3)]; %change from Jup Sys III to EPHIO
B_europa_prime=B_europa_ephio;
B_europa_prime(:,3)=zeros(size(B_europa_ephio(:,1)));

%calculation of seconday field
M=induction(r_traj, sigma,  h(q), d, B_europa_prime, omega);


constant=mu_0/(4*pi);

for n=1:size(r_traj)
    rnorm(n)=sqrt(r_traj(n,1).^2+r_traj(n,2).^2+r_traj(n,3).^2);
```

```
88  end
89
90  rnorm=rnorm';
91  r2=rnorm.^2;
92  r5=rnorm.^5;
93  rdotM=dot(r_traj,M,2);
94
95  %secondary field at space craft
96  for n=1:size(r_traj)
97
98      B_s(n,:)=(constant.*((3.*rdotM(n).*r_traj(n,:))-(r2(n).*M(n,:)))./
            r5(n);
99
100 end
101
102 B_s=[B_s(:,1) B_s(:,2) B_s(:,3)];
103
104
105 %Calculation of empirical B-field from linear fit of data
106 P1 = polyfit(data_ephio(:,1),data_ephio(:,2),1);
107 P2 = polyfit(data_ephio(:,1),data_ephio(:,3),1);
108 P3 = polyfit(data_ephio(:,1),data_ephio(:,4),1);
109
110 B1 = data_ephio(:,1).*P1(1) + P1(2);
111 B2 = data_ephio(:,1).*P2(1) + P2(2);
112 B3 = data_ephio(:,1).*P3(1) + P3(2);
113
114 %the primary field at the space craft
115
116 B_p = [B1 B2 B3];
117
118
119 %total theoretical field
120 B_sum=B_p+B_s;
121
122 %length of total field
123 B_abs=sqrt(B_sum(:,1).^2+B_sum(:,2).^2+B_sum(:,3).^2);
124
125 %re-scale of time
126 time=time/(3600*24);
127 time=time+t0;
128
129 %plot of model for different conductivities
130
131
132
133 subplot(3,1,1)
134 l=plot(time, B_sum(:,1));
135 legends{q} = sprintf(['Shell thickness ' num2str(h(q)) ' [m]']) ;
136 hold on
137 datetick
138 grid on
139
140 xlabel('Time [h]')
141 ylabel('Magnetic field strength [nT]')
142 title("The modelled field for different shell thicknesses for the "+
        flyby+" flyby in the x-direction")
143
```

```
subplot(3,1,2);
plot(time, B_sum(:,2))
hold on
datetick
grid on

xlabel('Time [h]')
ylabel('Magnetic field strength [nT]')
title("The modelled field for different shell thicknesses for the "+
    flyby+" flyby in the y-direction")

subplot(3,1,3);
plot(time, B_sum(:,3))
hold on
datetick
grid on

xlabel('Time [h]')
ylabel('Magnetic field strength [nT]')
title("The modelled field for different shell thicknesses for the "+
    flyby+" flyby in the z-direction")

end

legend(legends)
```

6.2.8 Script to plot the flybys relative Europa

```
%plot traajectory of space craftt in 3D for the differentt flybys

E4= read_galileo_MAG(4,'EPHIO');
%    EPHIO: time Bx By Bz |B|[nT] X_RE Y_RE Z_RE

E11= read_galileo_MAG(11,'EPHIO');
E12= read_galileo_MAG(12,'EPHIO');
E14= read_galileo_MAG(14,'EPHIO');
E15= read_galileo_MAG(15,'EPHIO');
E17= read_galileo_MAG(17,'EPHIO');
E19= read_galileo_MAG(19,'EPHIO');
E26= read_galileo_MAG(26,'EPHIO');

rx_4=E4(:,6);
ry_4=E4(:,7);
rz_4=E4(:,8);

rx_11=E11(:,6);
ry_11=E11(:,7);
rz_11=E11(:,8);

rx_12=E12(:,6);
ry_12=E12(:,7);
rz_12=E12(:,8);

rx_14=E14(:,6);
ry_14=E14(:,7);
rz_14=E14(:,8);

rx_15=E15(:,6);
ry_15=E15(:,7);
```

```
rz_15=E15(:,8);

rx_17=E17(:,6);
ry_17=E17(:,7);
rz_17=E17(:,8);

rx_19=E19(:,6);
ry_19=E19(:,7);
rz_19=E19(:,8);

rx_26=E26(:,6);
ry_26=E26(:,7);
rz_26=E26(:,8);

sphere
hold on

plot3(rx_4, ry_4, rz_4,'r')
plot3(rx_11, ry_11, rz_11,'--r')
plot3(rx_12, ry_12, rz_12,'g')
plot3(rx_14, ry_14, rz_14,'--g')
plot3(rx_15, ry_15, rz_15,'k')
plot3(rx_17, ry_17, rz_17,'--k')
plot3(rx_19, ry_19, rz_19,'b')
plot3(rx_26, ry_26, rz_26,'--b')

xlabel('r_x')
ylabel('r_y')
zlabel('r_z')
title('The trajectories of the flybys investigated, with Europa centered
    at [0,0,0]', 'fontsize', 25)
legend('Europa', 'E4', 'E11', 'E12', 'E14', 'E15', 'E17', 'E19', 'E26')
axis equal
```

6.2.9 Script to plot one flyby relative to Europa, in the xy-plane

```
%plot orbit of space craft


%read data
data_ephio = read_galileo_MAG(26,'EPHIO');
%    EPHIO: time Bx By Bz |B|[nT] X_RE Y_RE Z_RE

data_sys3 = read_galileo_MAG(26,'SYS3');
%    SYS3:  time Br Btheta Bphi |B|[nT] R[R_E] Lat[deg] ELong[deg] Wlong
    [deg]

flyby='E26';

rx=data_ephio(:,6);
ry=data_ephio(:,7);
rz=data_ephio(:,8);


center=[0 0];
radius=1;
c=viscircles(center,radius);
hold on
plot(rx,ry)
```

```
23 plot(rx(1), ry(1),'*')
24 hold off
25
26 xlabel('X_{EPHIO}')
27 ylabel('Y_{EPHIO}')
28 title("Trajectory of space craft relative to Europa for "+flyby+"" , '
       fontsize', 25)
29 grid on
30 legend
31
32 axis equal
```